Active Galactic Nuclei

History

1908: E. Fath: Emission lines in NGC 1068

1926: E. Hubble: ditto in NGC 1068, 4051, 4151

1943: C. Seyfert: Recognization of galaxies with emission lines as class

1954: W. Baade & R. Minkowski: Cyg A is radio source

1963: M. Schmidt: 3C273 has $z = 0.158$

1963: J. Greenstein & Th. Matthews: 3C48 has $z = 0.368$

1985: R. Antonucci & J. Miller: Spectropolarimetry of NGC 1068

Major properties:

$\Longrightarrow$ very luminous ($L \sim 10^{12}\,L_{\odot}$)

$\Longrightarrow$ Mass of BH: $M \sim 10^{7\ldots8} M_{\odot}$

IAAT

Seyfert Galaxies, I

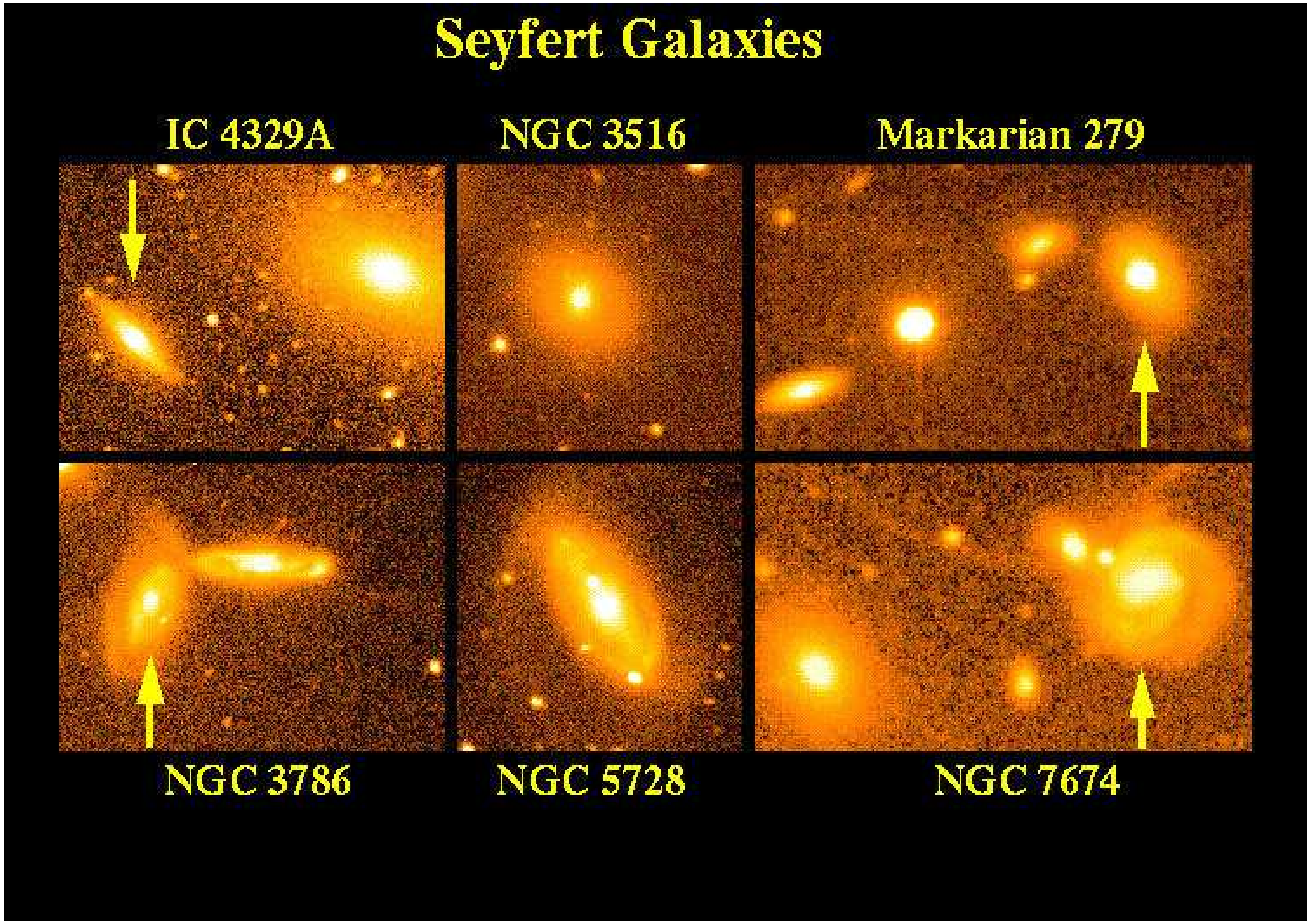

Seyfert Galaxies, II

$\Longrightarrow$ Emission lines from point-like center of galaxy, many ionization stages observable

Classification in gory detail:
Lawrence (1987)
Urry & Padovani (1995)

Radio-quiet AGNs:

Seyfert 1: pointlike nucleus, strong continuum from IR to X, broad allowed lines (H I, He I, He II, FWHM: 1000...5000 km/s), narrow forbidden lines (O III, N II, S II, FWHM $\sim$ 500 km/s)

Seyfert 2: weak continuum, both forbidden and allowed lines have FWHM$\sim$ 500 km/s

IAAT

Seyfert Galaxies, III

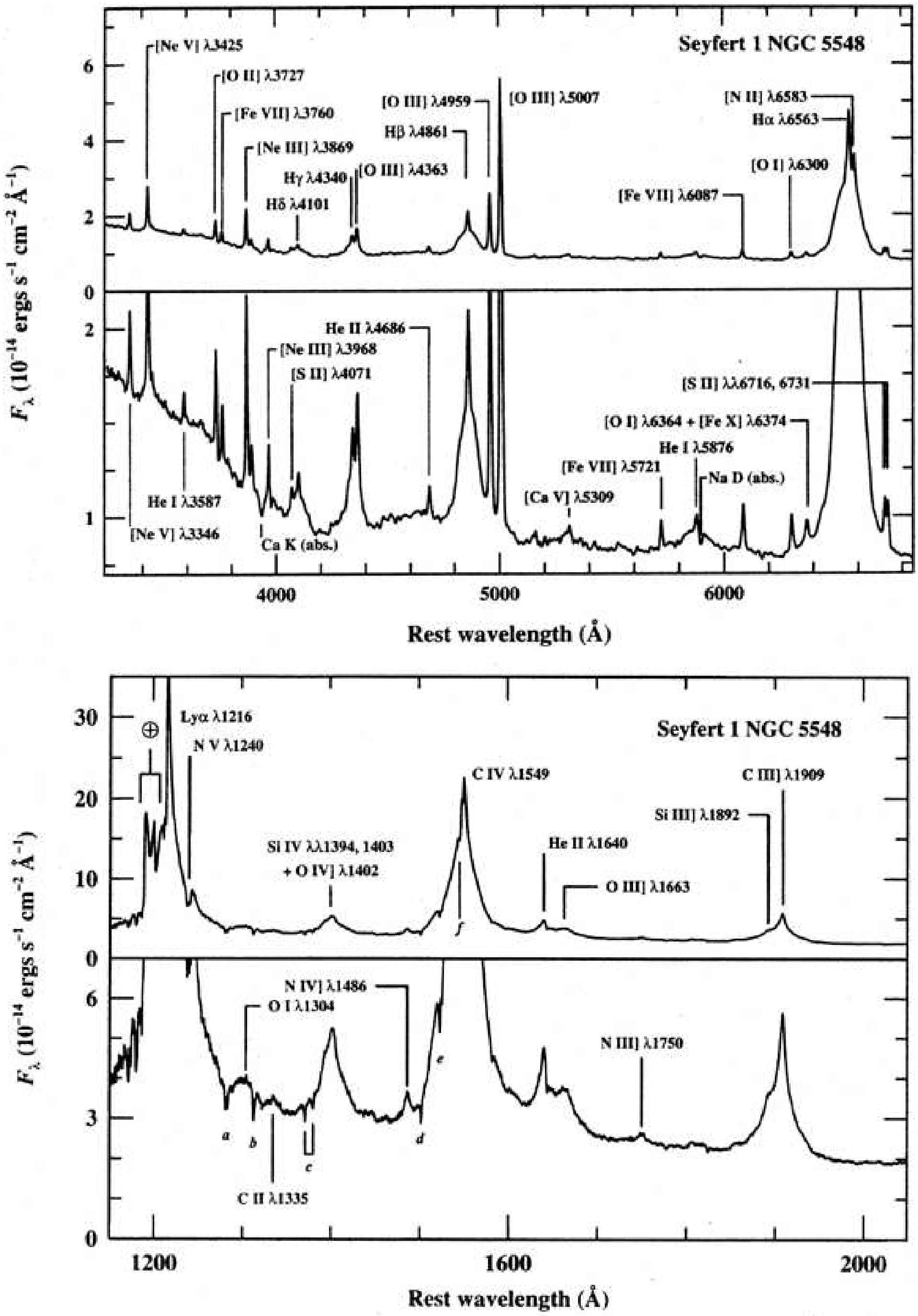

Peterson (1997)

Optical/UV spectrum of NGC 5548: a typical Seyfert 1 Galaxy.

Seyfert Galaxies, IV

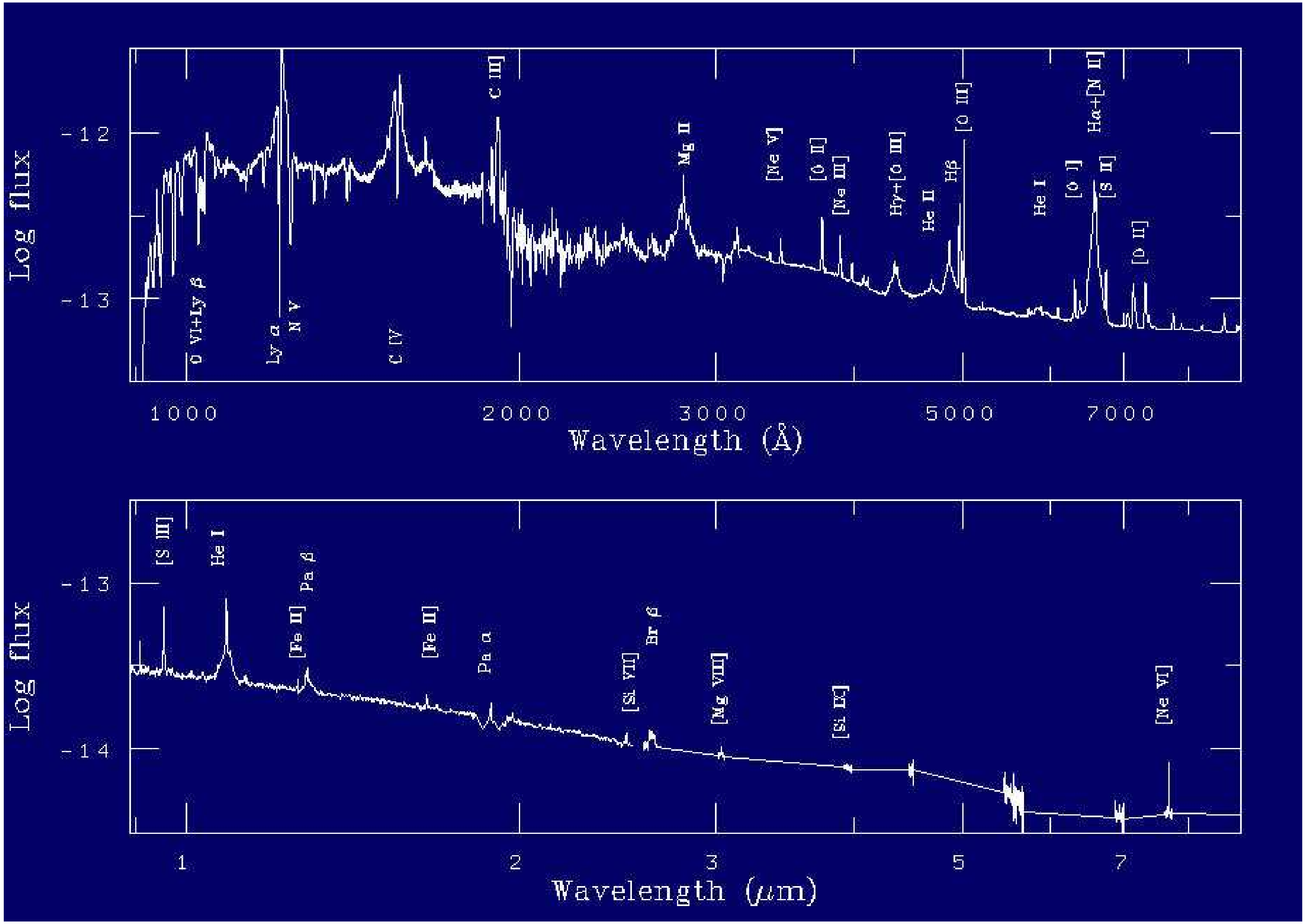

W. Keel: NGC 4151: another Seyfert 1 Galaxy

Seyfert Galaxies, V

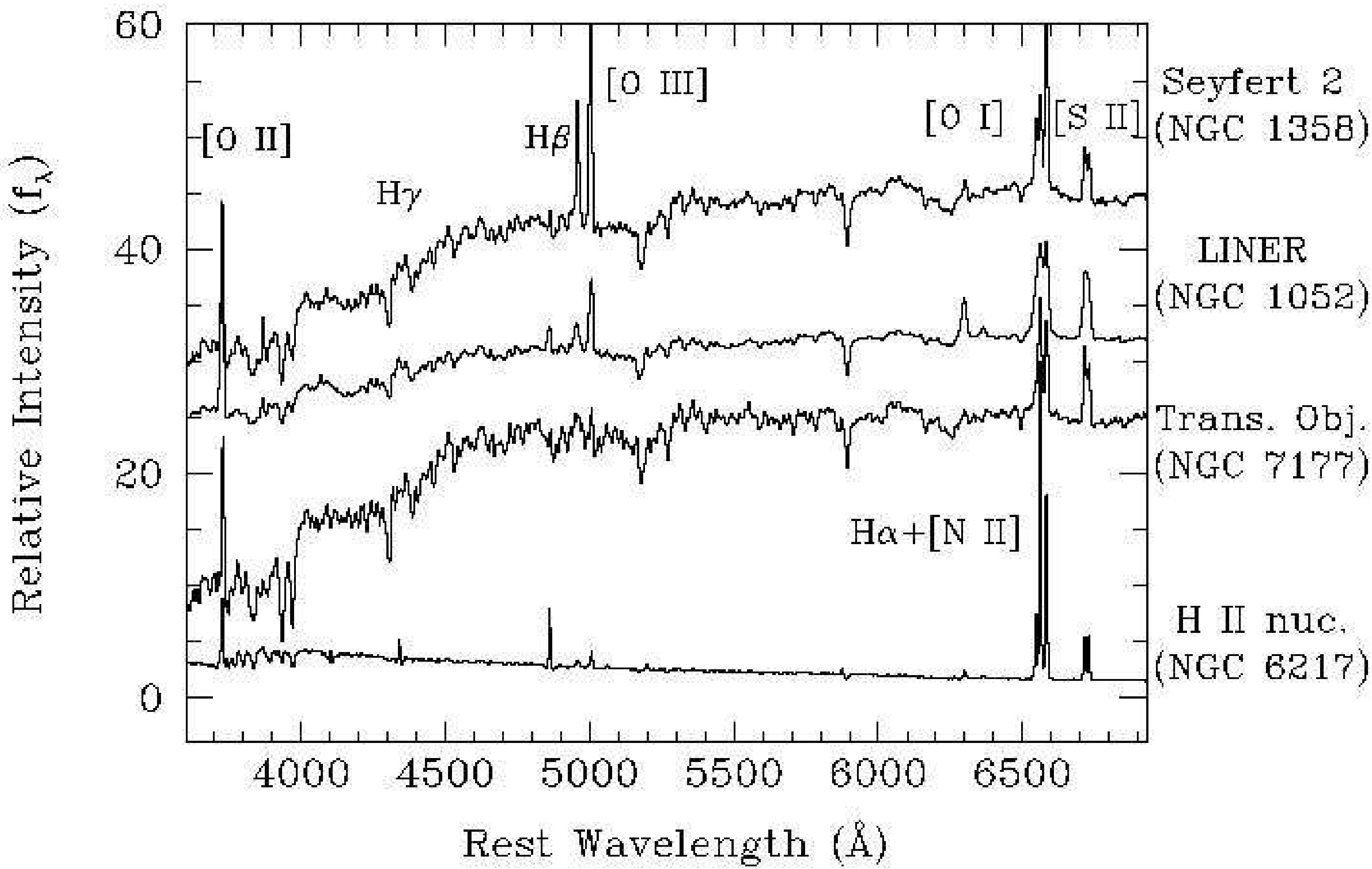

Ho, 1996

Seyfert 2 spectrum and sources with similar spectra

Seyfert Galaxies, VI

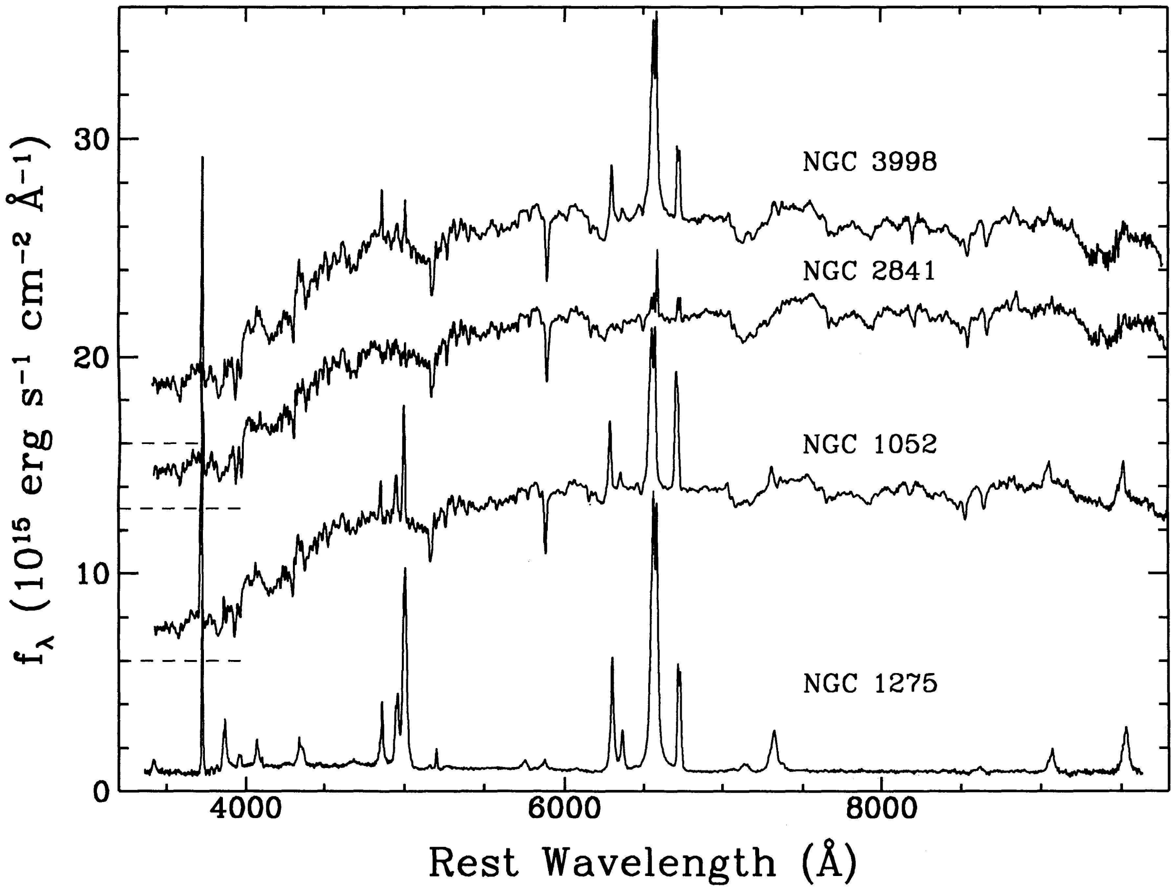

Ho et al., 1993

LINER (Low-Ionization Nuclear Emission Line Region galaxies): optical spectrum very similar to Seyfert 2 galaxies,

[O I] λ6300, [N II] $\lambda\lambda$6548, 6583 relatively strong.

IAAT

Seyfert Galaxies, VII

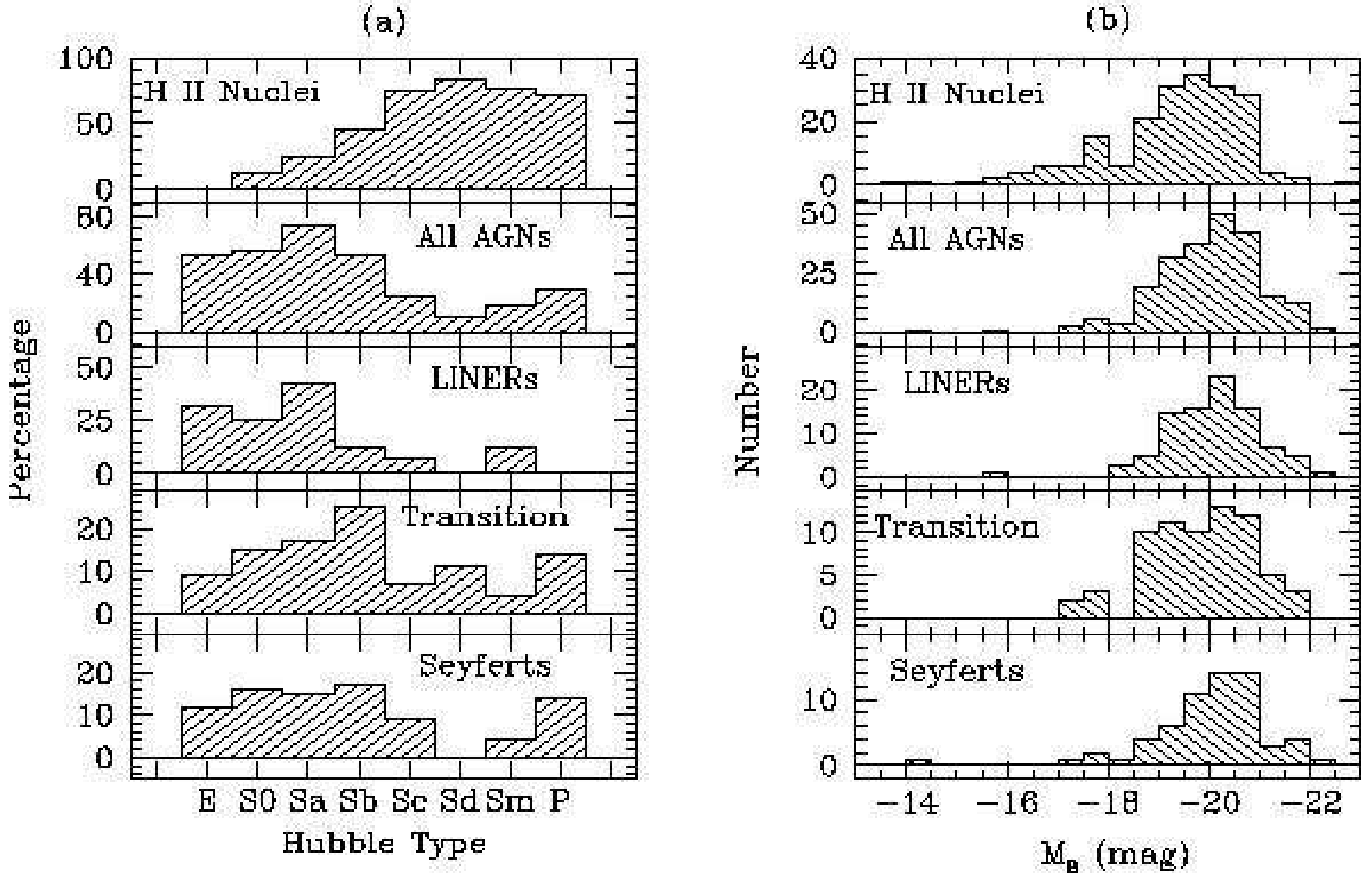

Ho, 1996

Seyferts are predominantly found in spiral galaxies (Sa, Sb).

Seyfert Galaxies, VIII

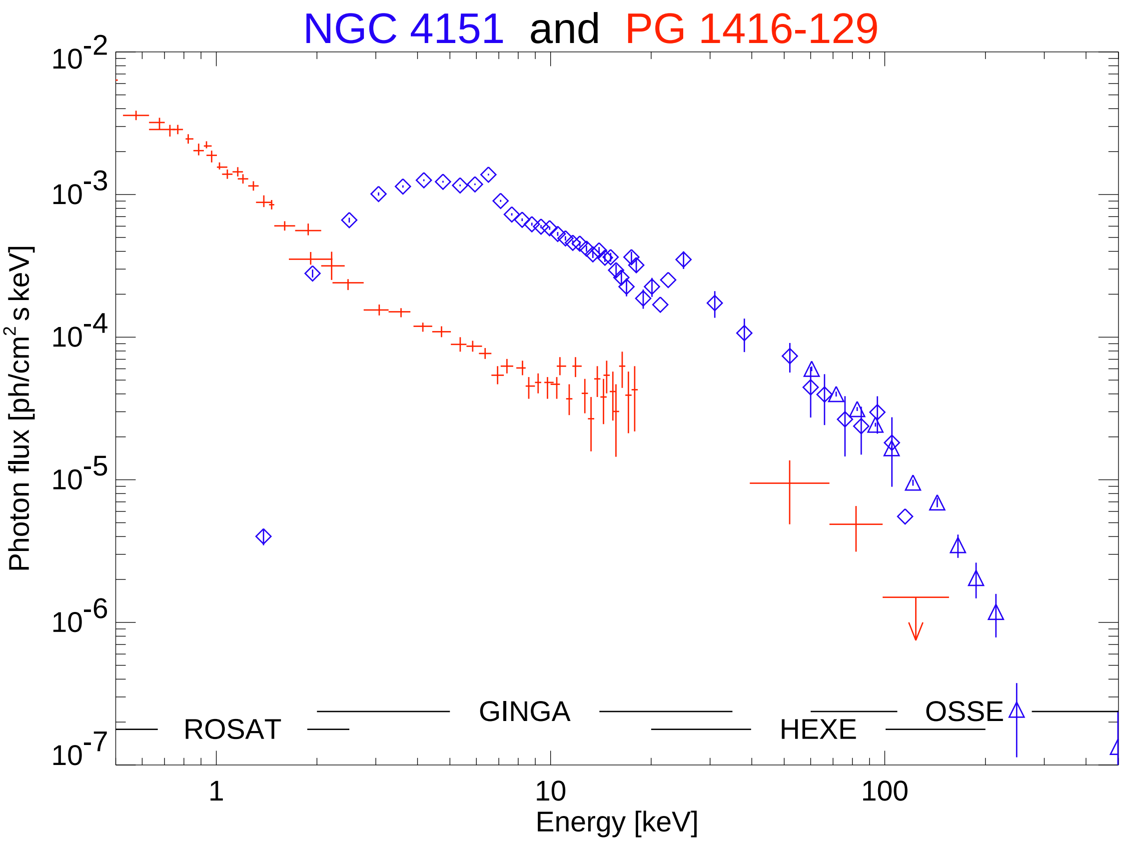

X-ray spectrum similar to galactic Black Holes

- $N_{\mathrm{ph}}(E) \propto E^{-\Gamma}$, where $\Gamma \sim 0.7 \ldots 1$
- Exponential cutoff at around 100 keV.

$\Longrightarrow$ Due to Comptonization; indication of hot material close to the BH

- Fe-edge
- Kα-line with EW=160...300 eV at 6.4 keV
- Steepening above 10 keV

$\Longrightarrow$ Due to Compton reflection; indication of cold material close to the BH

Seyfert Galaxies, IX

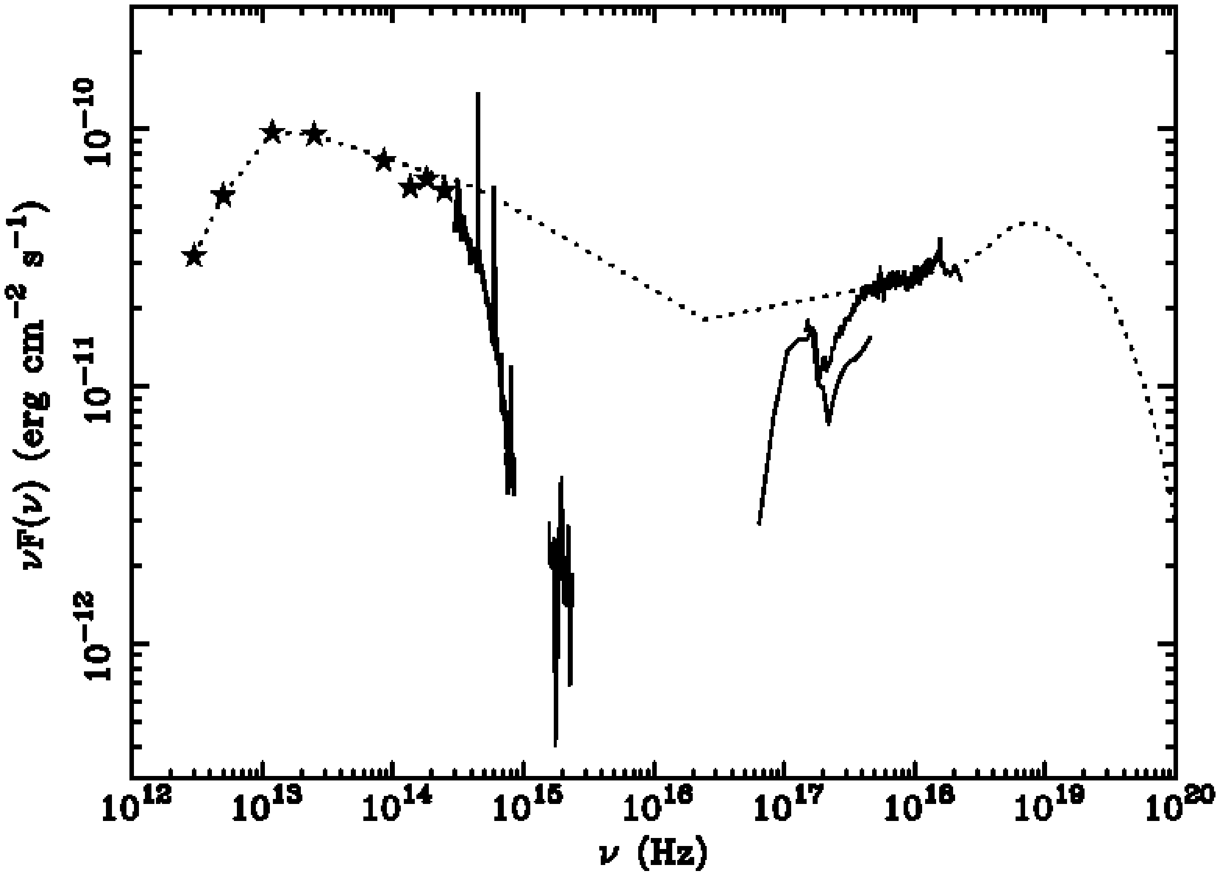

MCG−6-30-15 spectral energy distribution (Reynolds et al.)

Spectra well explained by thermal emission from accretion disk plus Comptonization

IAAT

Radio Loud Galaxies

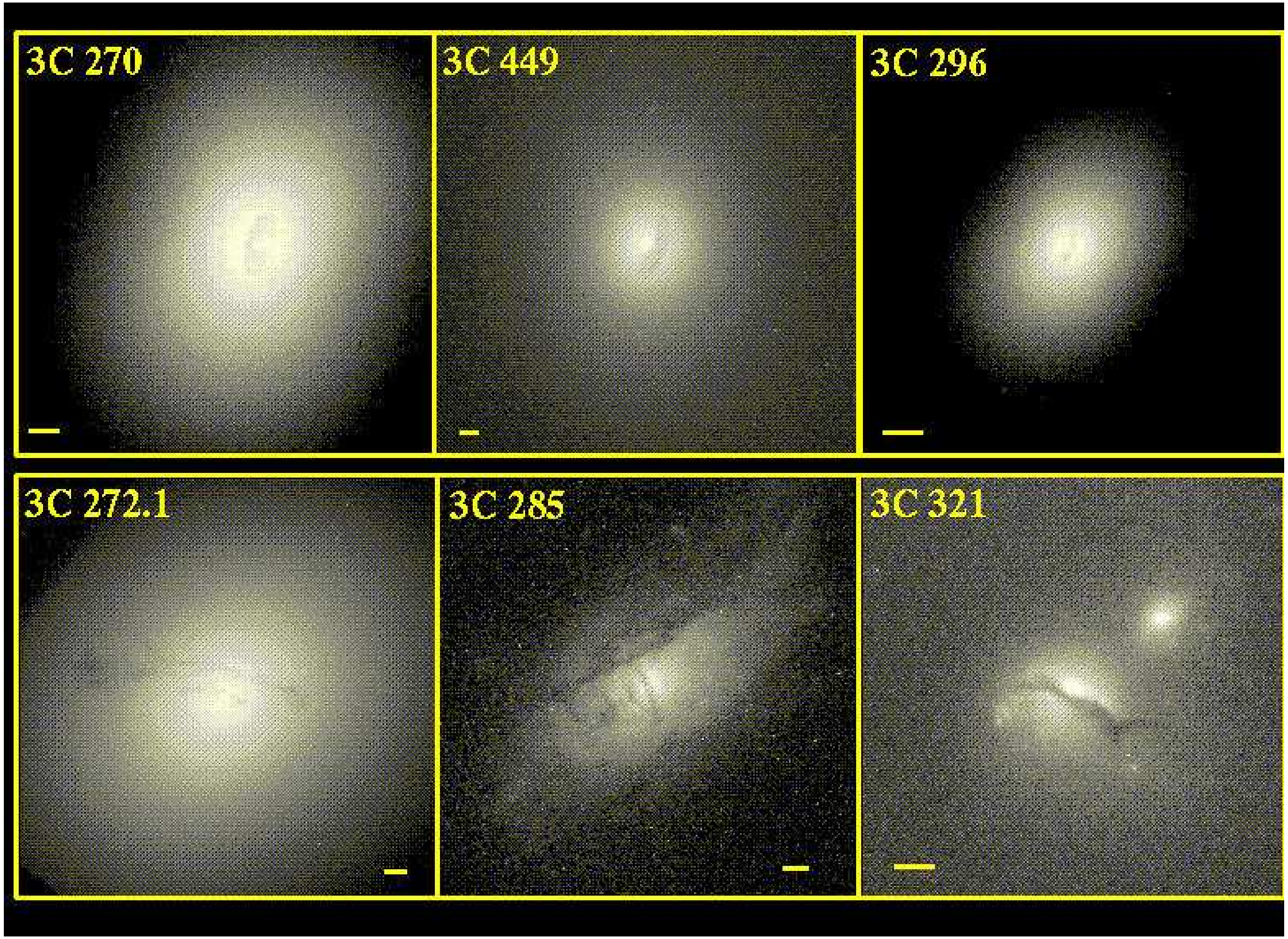

Radio loud galaxies are often found in ellipticals

Radio Loud Galaxies

Radio Loud Galaxies show jets.

Classification: Fanaroff-Riley Classes

FR 1: • nucleus dominates
- less luminous
- bright
- broad jets ending in plumes
- two asymmetric jets

FR 2: • luminous radio sources
- lobes dominate
- weak jets ending in radio lobes

Radio Loud Galaxies

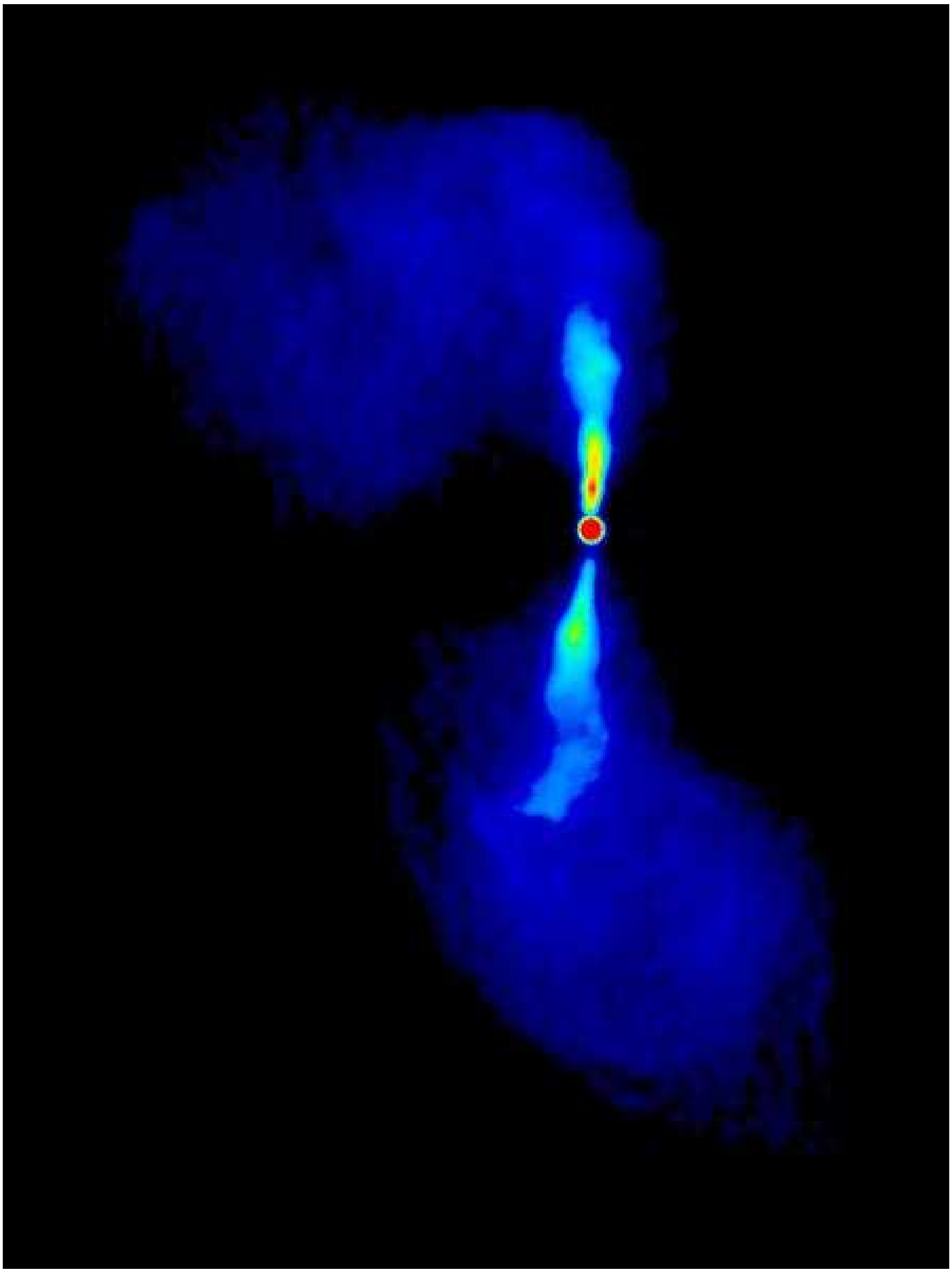

Laing & Bridle (1997); VLA 4885 MHz, $134'' \times 170''$

Radio image of M84 (3C272.1):

A typical FR 1 galaxy

Radio Loud Galaxies

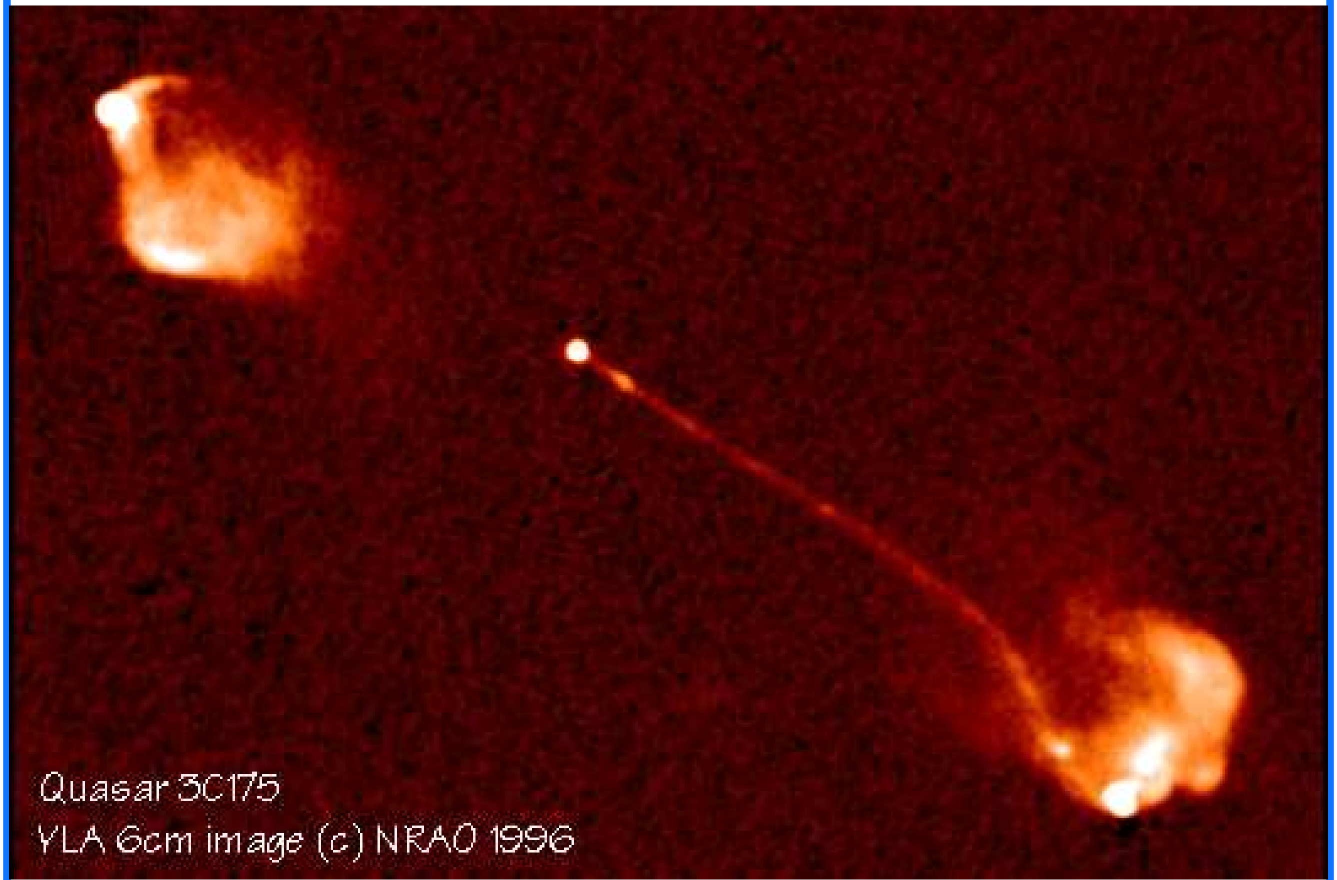

A. Bridle (priv. comm.)

Radio image of 3C175 ($z = 0.768$):
A typical FR 2 galaxy

one sided jet

Edge brightening $\Longrightarrow$ Shock heating due to interaction with ambient intergalactic medium (IGM)

Radio Loud Galaxies

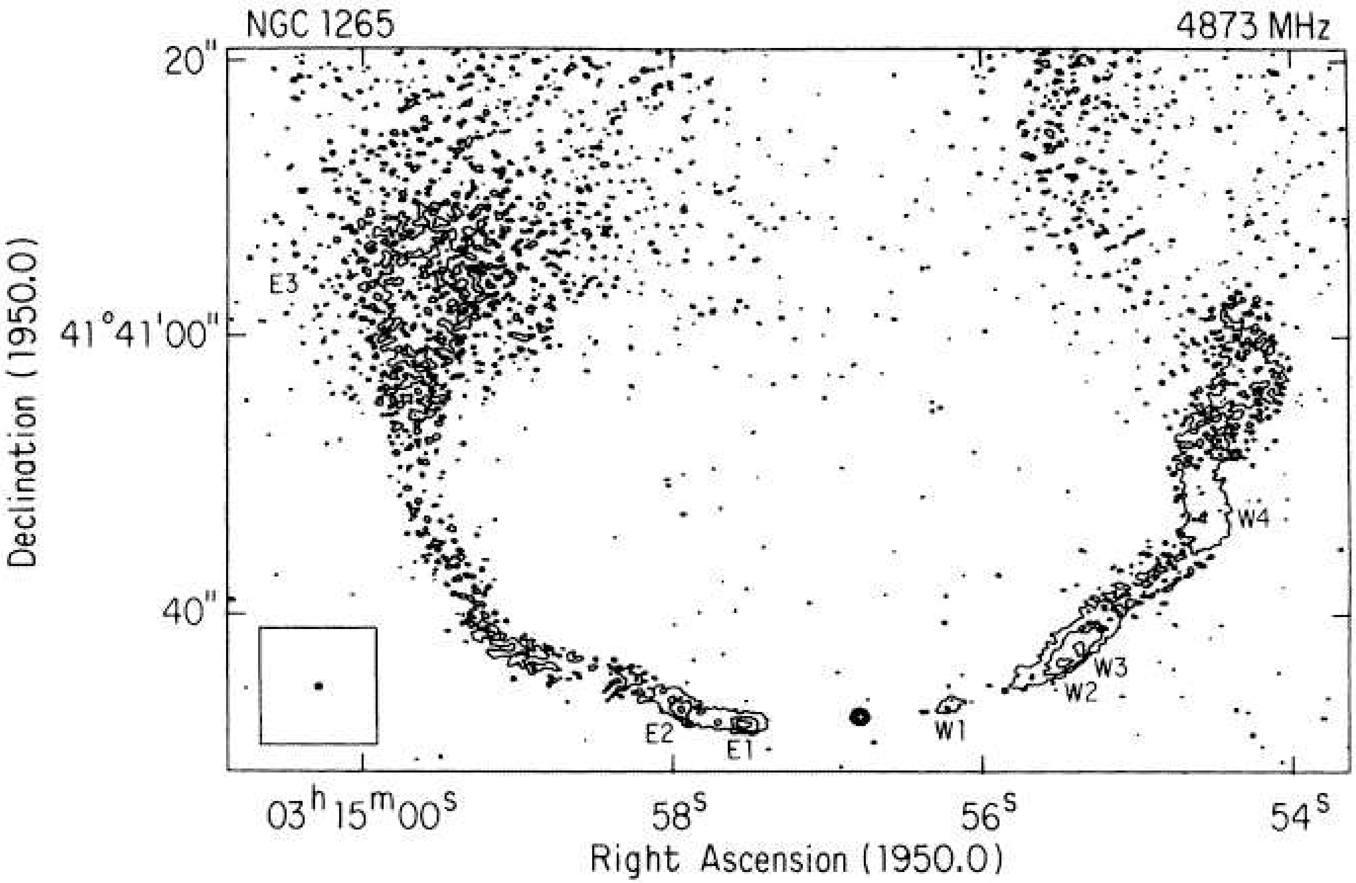

NGC 1265: a head-tail radio galaxy $\Longrightarrow$ Interaction with IGM. Sources of this type often found in galaxy clusters.

Radio Loud Galaxies

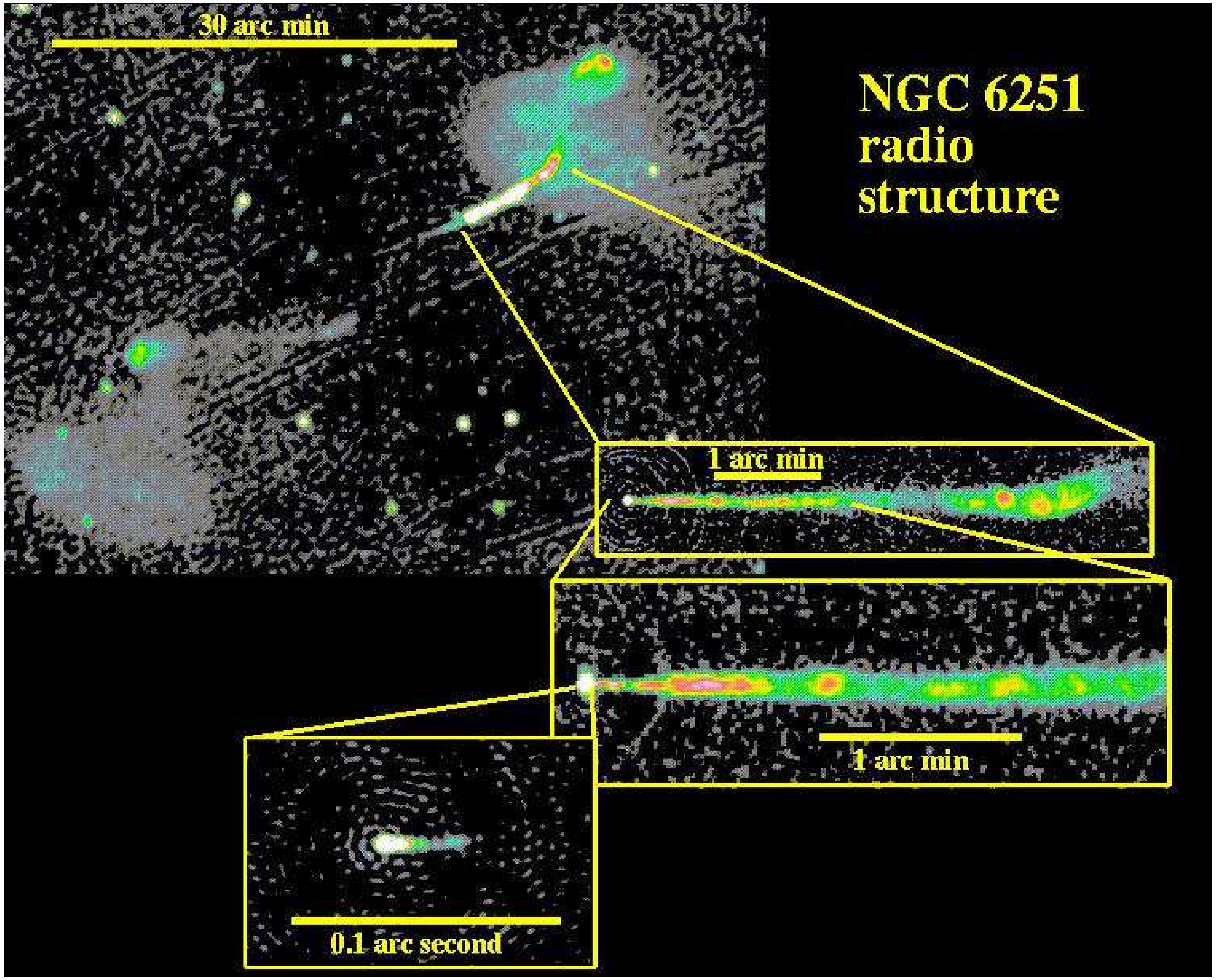

W. Keel; Jets are well collimated at all length scales

Radio Loud Galaxies

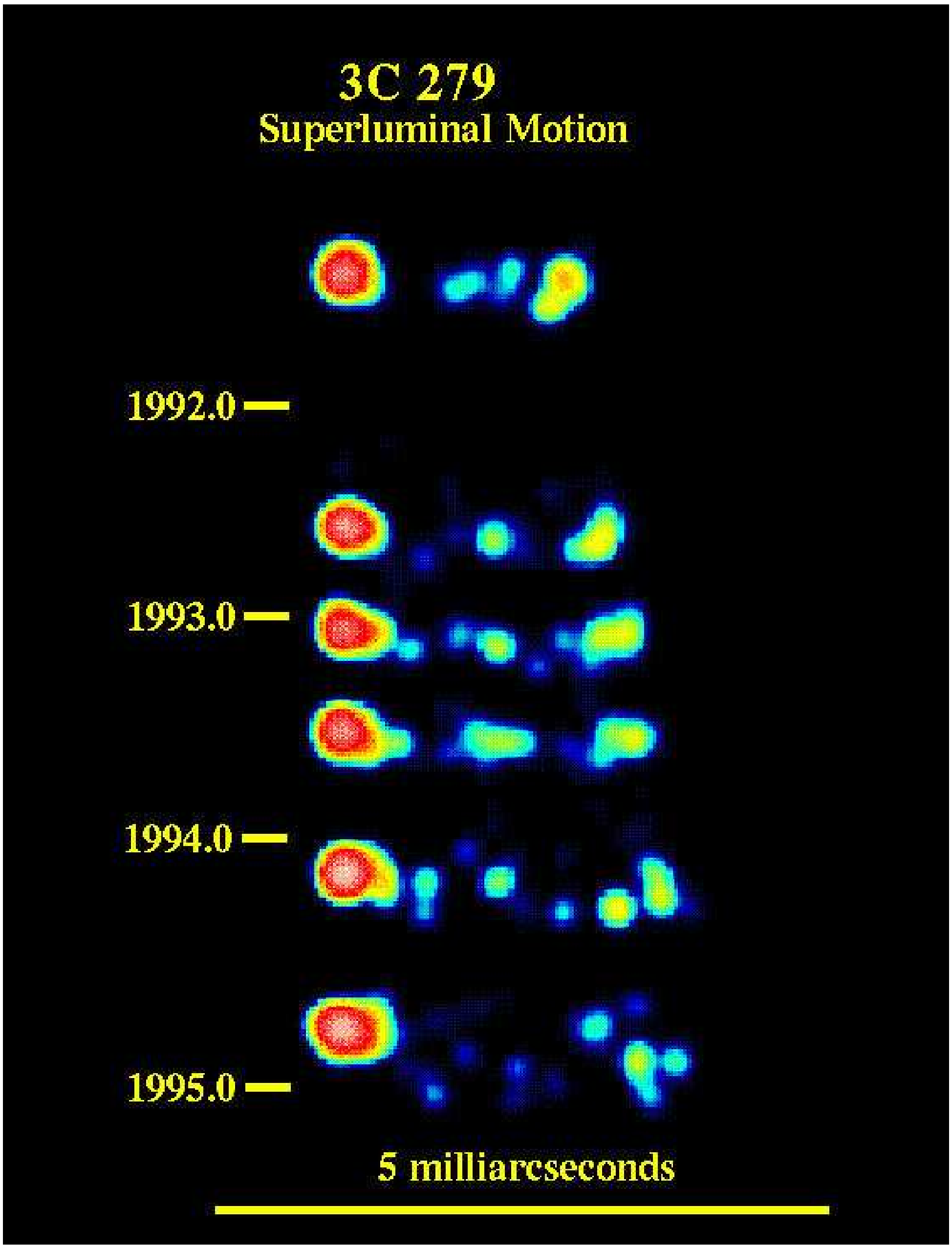

Superluminal motion in 3C279

Superluminal motion seen in many radio loud sources.

Explanation: see discussion in XRB chapter on superluminal motion in microquasars.

Radio Loud Galaxies

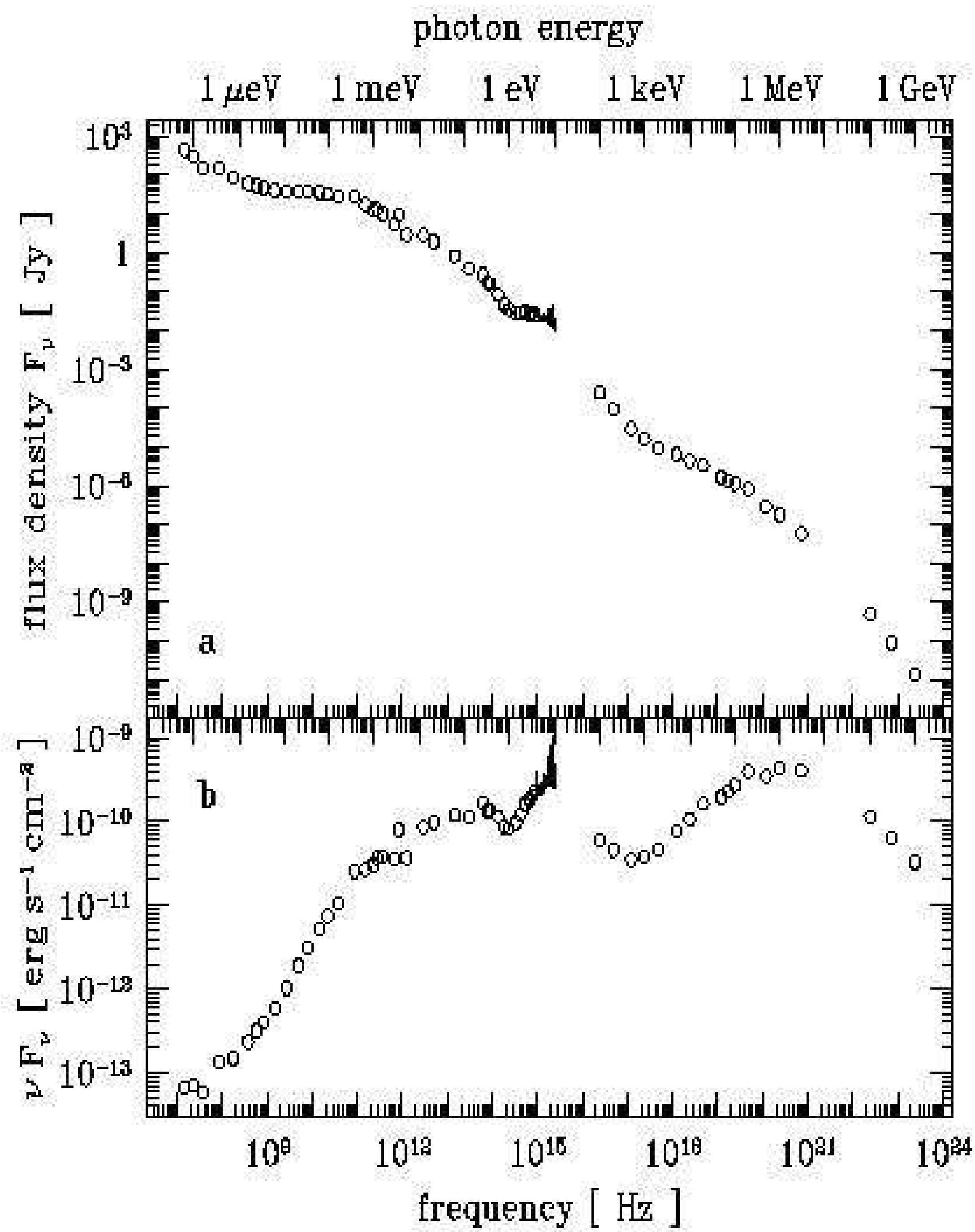

Courvoisier (1998): Spectral Energy Distribution of 3C 273

νf_ν-plot gives energy per frequency decade

Radio Loud Galaxies

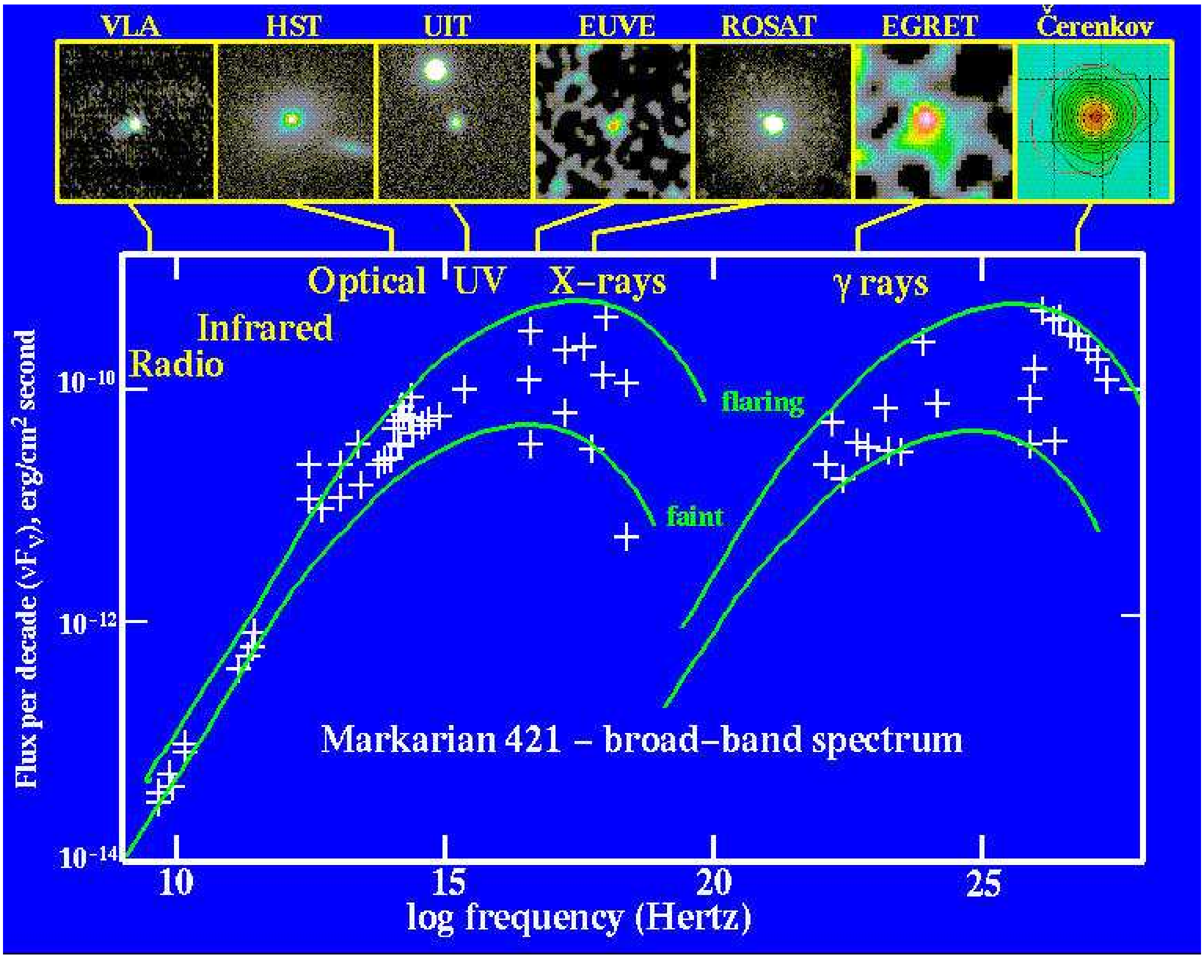

W. Keel

General model for broad band spectral energy distribution: Synchrotron-Self Compton radiation

Unifi ed Model

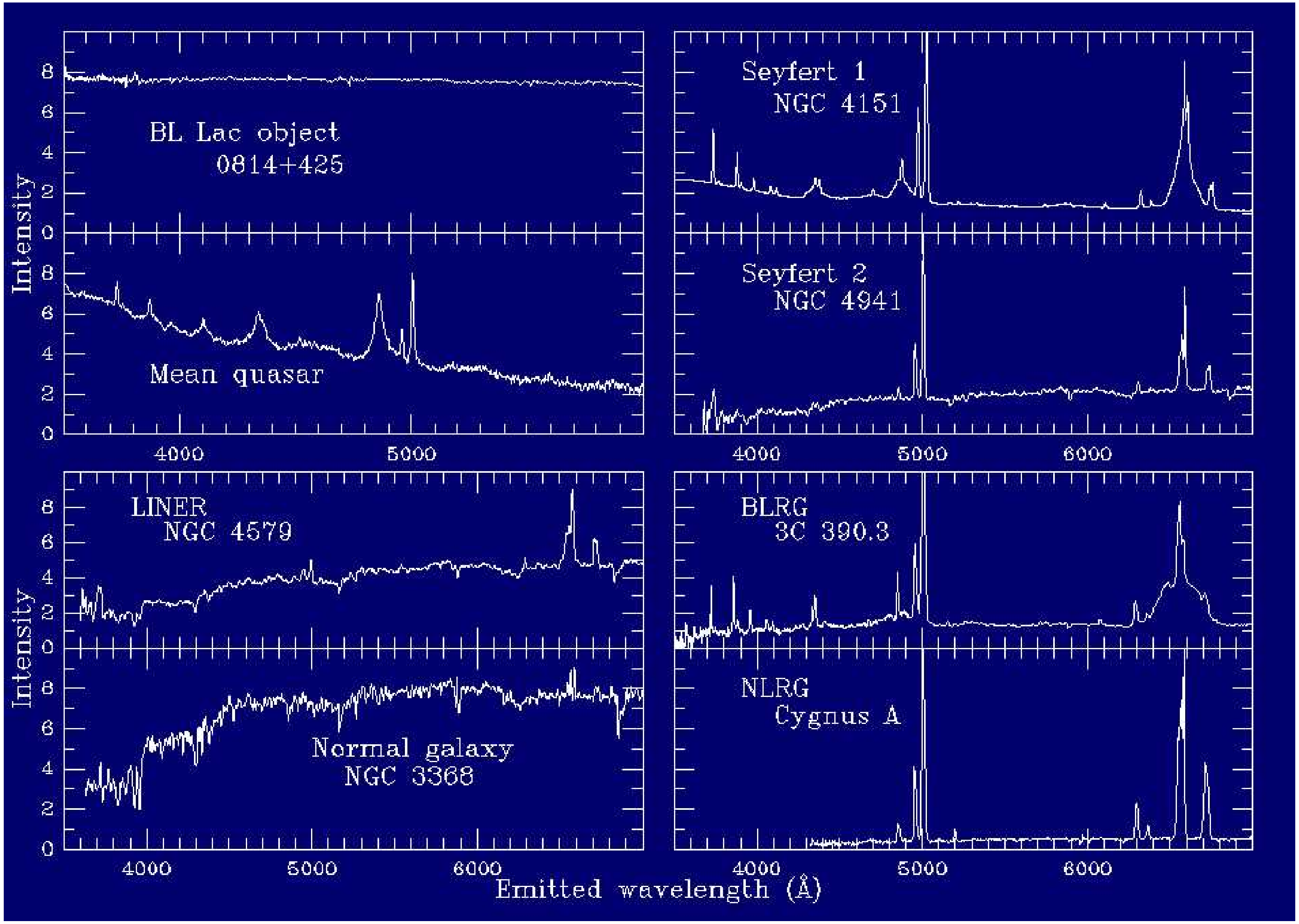

Summary of optical spectra of different AGN types

Unifi ed Model

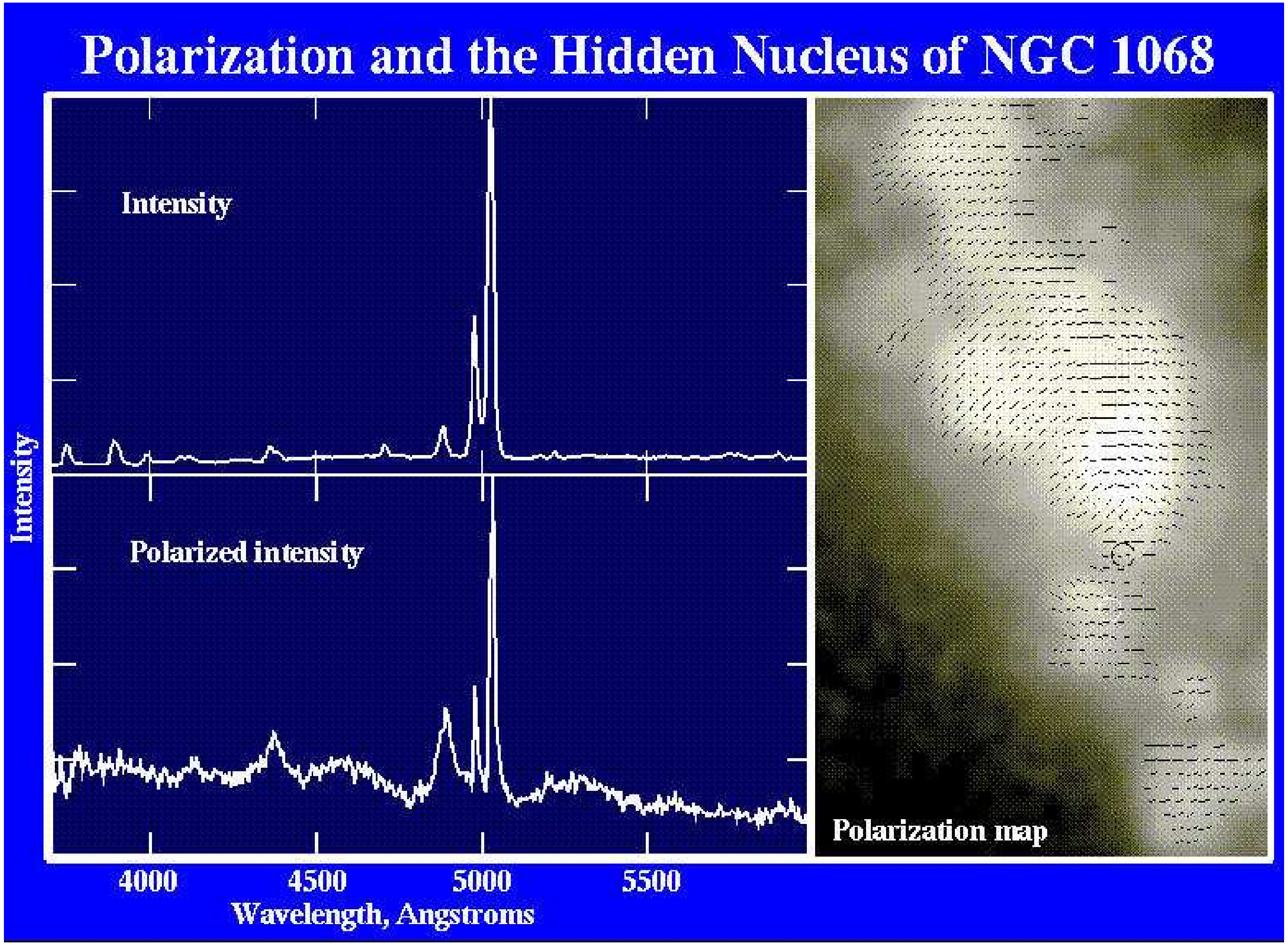

Antonucci & Miller: NGC 1068 (Sy 2) in polarized light shows broad lines $\Longrightarrow$ Same as Sy 1!

Unifi ed Model

The Unifying Model of AGN

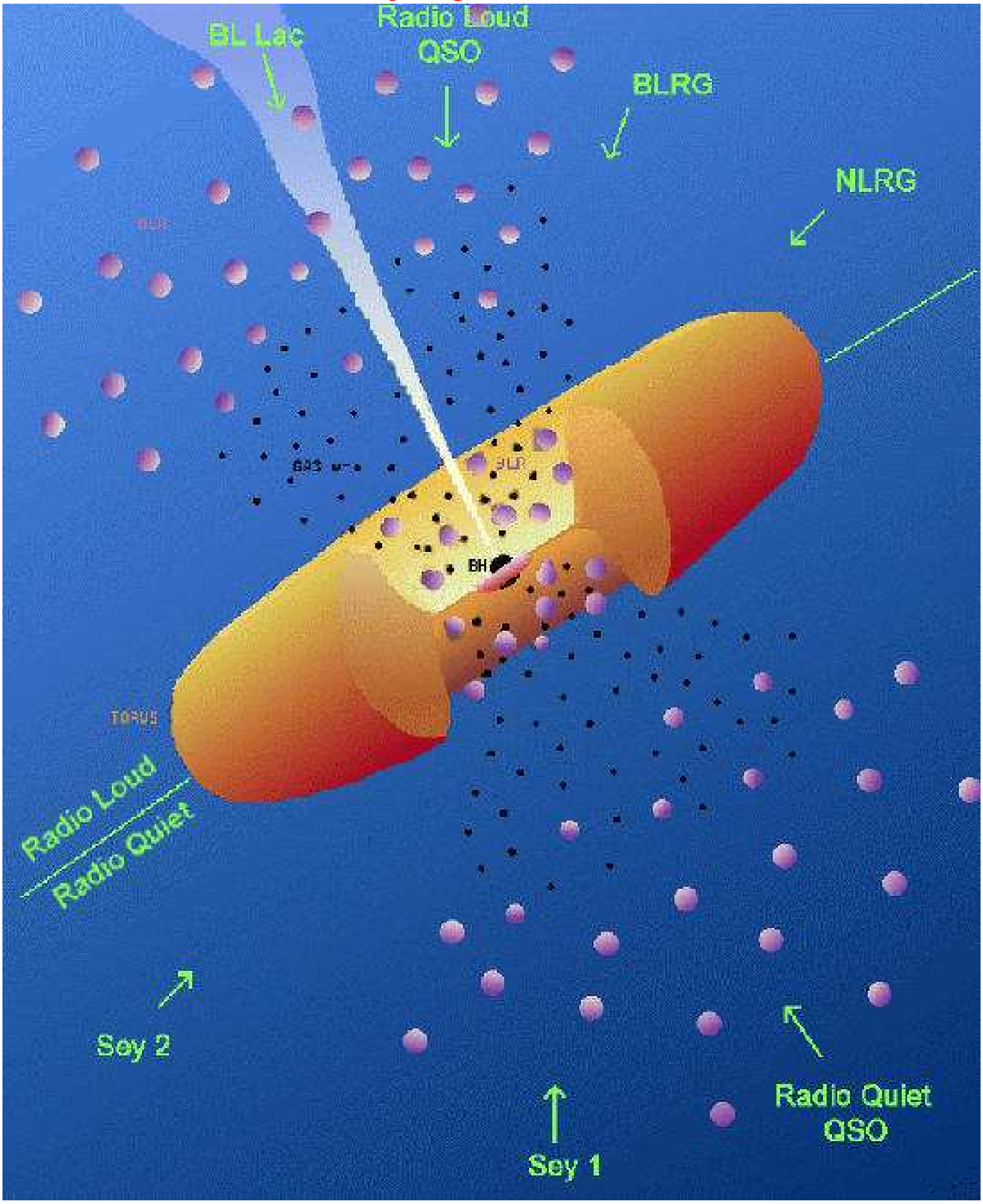

Urry & Padovani

IAAT

Introduction

Two types of AGN lines:

broad lines: : FWHM: $\Delta\nu/\nu \sim 0.05\ldots0.1$, i.e. $1000\ldots10000\,\mathrm{km\,s^{-1}}$

narrow lines: : FWHM: $\Delta\nu/\nu \sim 0.002\ldots0.1$, i.e. $\lesssim 100\,\mathrm{km\,s^{-1}}$

What is absorbing gas $\Longrightarrow$ Temperature? Density? Abundances?

Similarity of optical spectrum to planetary nebulae $\Longrightarrow$ photoionization!

Photoionization, I

Assume: cloud irradiated by photons

Goal: only source for ionization: photoionization

Equilibrium: number ionizations = number of recombinations

$$\int_{\nu_{\text{ion}}}^{\infty} a(\nu)\frac{F_\nu}{h\nu}N(X^r)\mathrm{d}\nu = \alpha(T)N_\mathrm{e}N(X^{r+1}) \tag{6.1}$$

where

$a(\nu)$: photoionization cross section (cm^2; $\propto E^{-3}$)

$\alpha(T_\mathrm{e})$: Recombination coefficient (cm^3 s^{-1})

N_i: particle density (cm^{-3})

F_ν: local photon flux, erg cm^{-2} s^{-1} keV^{-1},

$$F_\nu = \frac{L_\nu}{4\pi D^2} \tag{6.2}$$

Since $a(\nu)$ quickly decreasing function:

$$\frac{N(X^r)}{N(X^{r+1})} \sim \frac{a(\nu_{\text{ion}})}{\alpha(T)}\frac{L}{4\pi D^2 N_\mathrm{e}}\frac{1}{h\nu_{\text{ion}}} \tag{6.3}$$

i.e., ionization equilibrium mainly depends on

$$U = \frac{L/4\pi D^2 h\nu_{\text{ion}}}{N_\mathrm{e}}\frac{1}{c} = \frac{\text{\# ionizing photons/cm}^3}{\text{\# electrons/cm}^3} \tag{6.4}$$

the ionization parameter

many other definitions available!

Photoionization, II

In reality, other physical processes need to be considered:

Ionization:

- Photoionization
- collisional Ionization
- Auger-Ionization

Recombination: • radiative recombination

- dielectric recombination

Continuum Processes: • Bremsstrahlung

- Compton-Scattering

Solution using advanced radiation codes such as Cloudy or XSTAR

Line Diagnostics: Density, I

Choose atom with two levels with almost same excitation energy. Either radiative or collisional deexcitation.

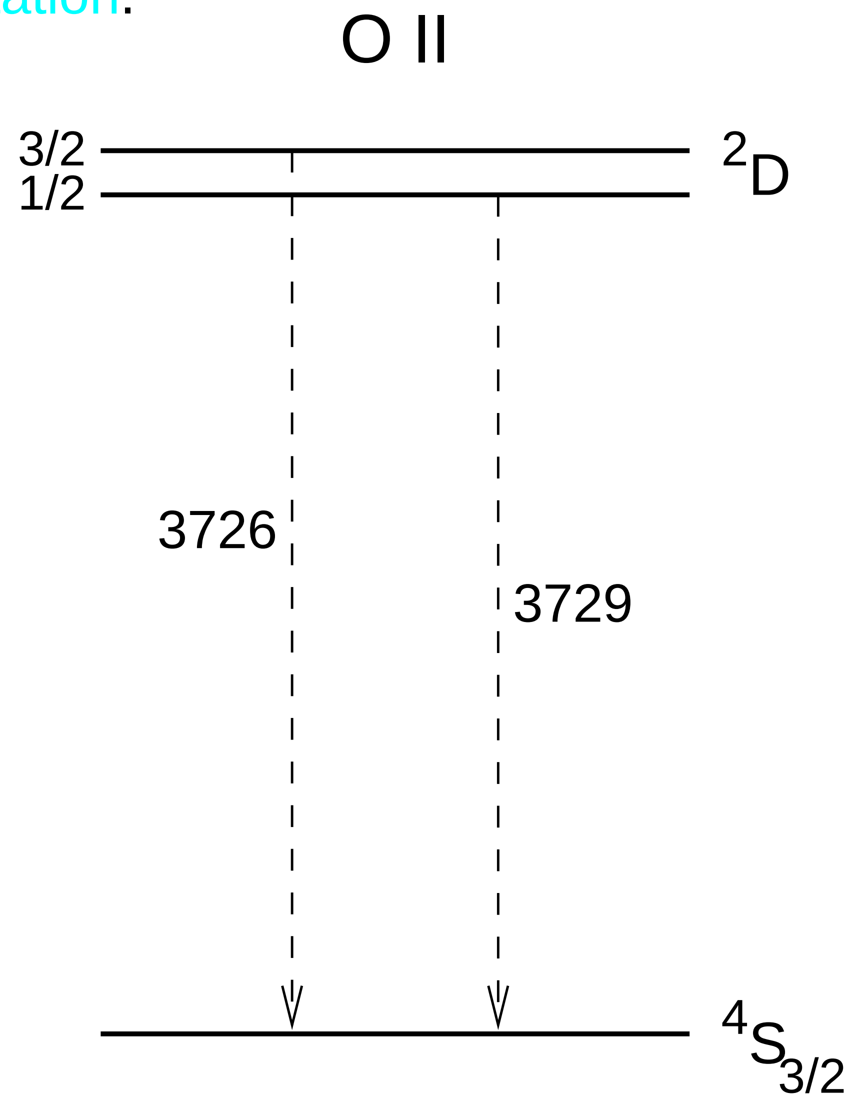

For $N_\mathrm{e} \approx 1000\,\mathrm{cm}^{-3}$ use [O II] 3729/3726, for higher densities: C II

Line Diagnostics: Density, II

Rate equations in equilibrium:

$$n_1 n_e C_{12} = n_2 A_{21} + n_2 n_e C_{21} \tag{6.5}$$

$$n_1 n_e C_{13} = n_3 A_{31} + n_3 n_e C_{31} \tag{6.6}$$

where A_{ij} Einstein-Coeffi cient, C_{ij} coeffi cient for collisional (de)excitation.

Computation of C_{ij}:

For de-excitation:

$$C_{21} = \int_0^\infty \sigma_{21}(v) v f(v) \mathrm{d}^3 v \tag{6.7}$$

where σ: cross section, $f(v)$ Maxwell.

One can show that

$$\sigma_{21}(v) = \frac{\pi \hbar^2}{m^2 v^2} \frac{\Omega_{21}}{g_2} \tag{6.8}$$

where Ω_{21}: collision strength.

Therefore

$$C_{21} = \frac{\hbar^2}{m^{3/2}} \frac{\Omega_{21}}{g_2} \left(\frac{2\pi}{kT}\right)^{1/2} \sim \frac{8.616 \times 10^{-6}}{T^{1/2}} \frac{\Omega_{21}}{g_2} \mathrm{cm}^3\,\mathrm{s}^{-1} \tag{6.9}$$

Because of Microreversibility

$$C_{12} = \frac{g_2}{g_1} C_{21} \exp(-E_{12}/kT) \tag{6.10}$$

Line Diagnostics: Density, III

Solve rate equations

$$\frac{n_2}{n_1} = \frac{n_e C_{12}}{A_{21} + n_e C_{21}} \qquad (6.11)$$

$$= \frac{n_e}{A_{21} + n_e C_{21}} \frac{g_2}{g_1} C_{21} \exp(-E_{12}/kT) \qquad (6.12)$$

and a similar equation for n_3/n_1.

Intensity of the line (assuming cloud is optically thin)

$$I_{21} = \frac{A_{21} n_2 h\nu_{21}}{4\pi} \qquad (6.13)$$

Therefore

$$\frac{I_{21}}{I_{31}} = \frac{A_{21} n_2 h\nu_{21}/4\pi}{A_{31} n_3 h\nu_{31}/4\pi} \qquad (6.14)$$

since $\nu_{21} \sim \nu_{31} \ldots$

$$= \frac{A_{21} n_2}{A_{31} n_3} \qquad (6.15)$$

$$= \frac{C_{21}}{C_{31}} \frac{g_2}{g_3} \frac{A_{21}}{A_{31}} \frac{A_{31} + n_e C_{31}}{A_{21} + n_e C_{21}} \exp(-E_{32}/kT) \qquad (6.16)$$

$$= \frac{g_2 C_{21}}{g_3 C_{31}} \frac{1 + n_e/n_{Cr,3}}{1 + n_e/n_{Cr,2}} \exp(-E_{32}/kT) \qquad (6.17)$$

where the critical density is defi ned by

$$n_{cr,2} = \frac{A_{21}}{C_{21}} \qquad (6.18)$$

Line Diagnostics: Density, IV

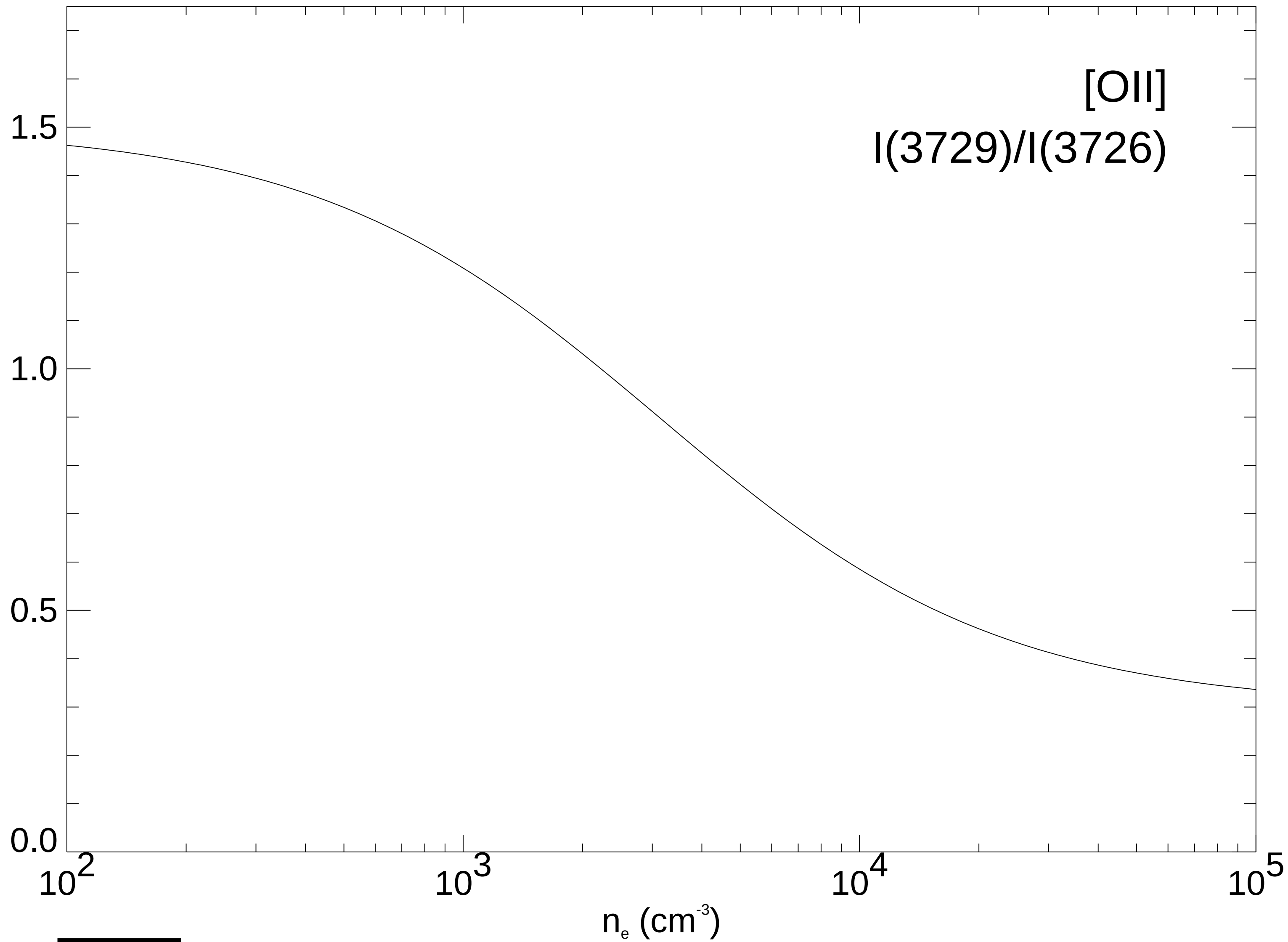

IAAT

Line Diagnostics: Temperature, I

To obtain temperature use similar ideas. This time, use two levels with different excitation energy

$\Longrightarrow$ Use different excitation probability of collisionial excitation

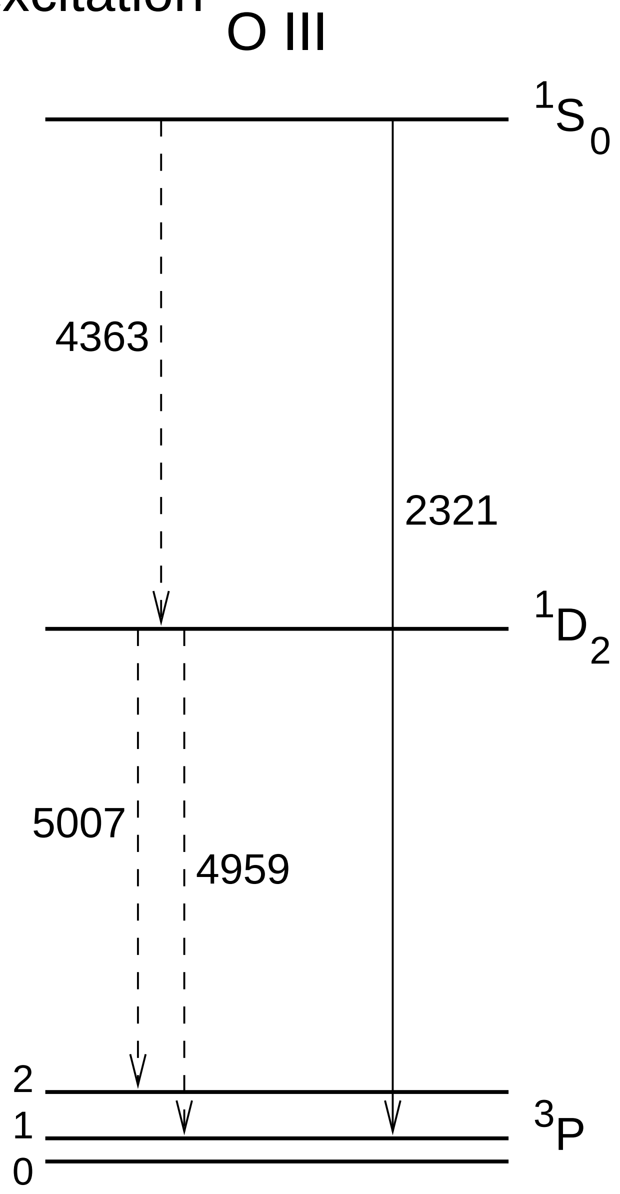

For $T \sim 10000\,\mathrm{K}$, mainly O III and N II

Line Diagnostics: Temperature, II

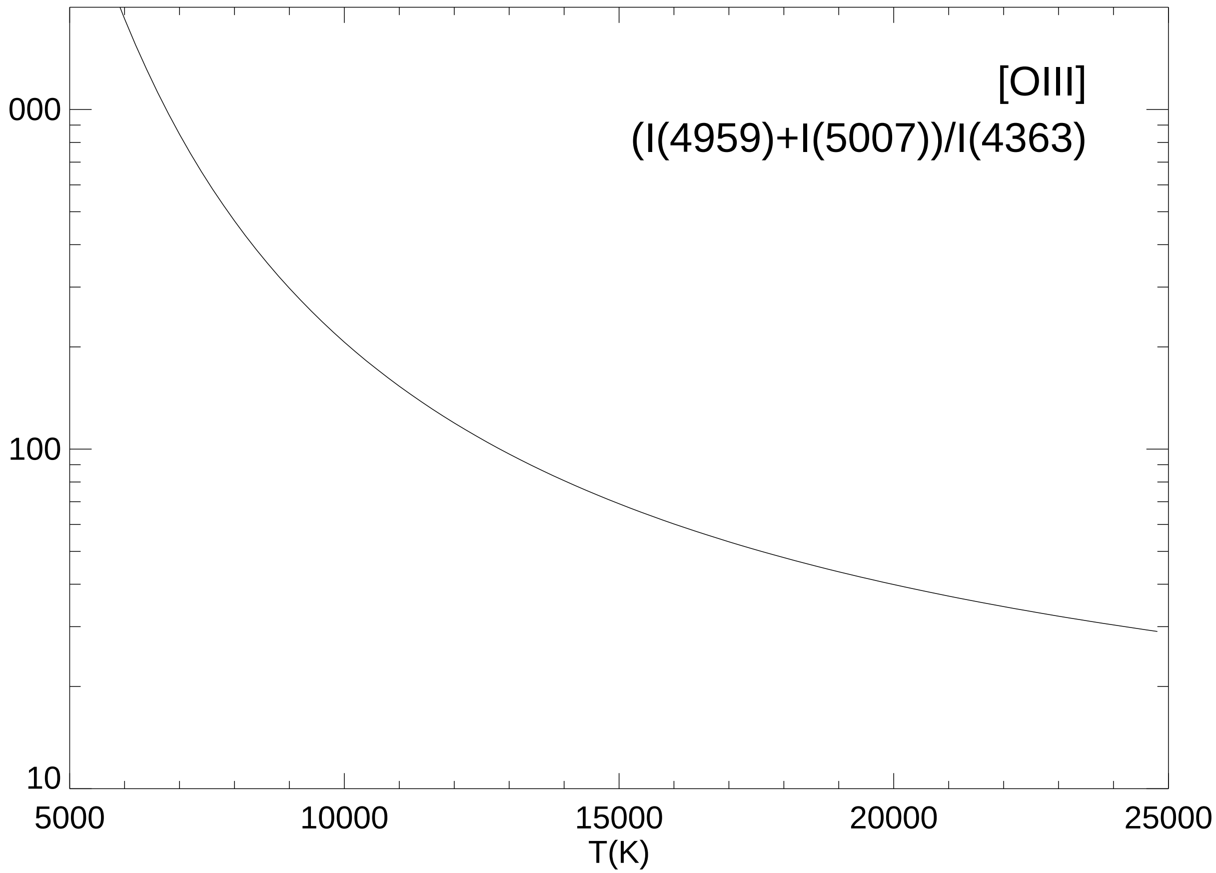

$$\frac{I(4959+5007)}{4363} = \frac{7.7\exp(3.29\times 10^4/T)}{1+4.5\times 10^{-4} n_\mathrm{e} T^{-1/2}} \tag{6.19}$$

IAAT

Mass determination

Mass determination: Determine number of emitting atoms from line strength.
Hydrogen: Hβ (less influenced by radiative transfer effects)

$$j_{\mathrm{H}\beta} = n_{\mathrm{e}} n_{\mathrm{p}} \alpha_{\mathrm{H}\beta} \frac{h\nu_{\mathrm{H}\beta}}{4\pi} \tag{6.20}$$

$$= \frac{n_{\mathrm{e}}^2}{4\pi} \alpha_{\mathrm{H}\beta}^{\mathrm{eff}} \frac{h\nu_{\mathrm{H}\beta}}{4\pi} \tag{6.21}$$

$$= 1.24 \times 10^{-25}\,\mathrm{erg\,s^{-1}\,cm^{-3}\,sr^{-1}} \frac{n_{\mathrm{e}}^2}{4\pi} \tag{6.22}$$

where $\alpha_{\mathrm{H}\beta}^{\mathrm{eff}}$: effective recombination coefficient for $n = 4 \to n = 2$ transition (weakly temperature dependent).
Total emissivity

$$L_{\mathrm{H}\beta} = \int\int j_{\mathrm{H}\beta}\,\mathrm{d}\Omega\,\mathrm{d}V \tag{6.23}$$

$$= \frac{4\pi n_{\mathrm{e}}^2}{3} \cdot 1.24 \times 10^{-25} r^3 f\,\mathrm{erg\,s^{-1}} \propto \int n_{\mathrm{e}}^2\,\mathrm{d}V \tag{6.24}$$

where $\int n_{\mathrm{e}}^2\,\mathrm{d}V$:emission measure, and f: filling factor.
Number of clouds:

$$N_{\mathrm{cloud}} l^3 = f r^3 \tag{6.25}$$

where l cloud radius, r: size of region

Results: NLR

Typical numbers for the NLR:

$$r = 19\,\mathrm{pc}\,\left(\frac{L_{41}(\mathrm{H}\beta)}{f n_3^2}\right)^{1/3} \tag{6.26}$$

For close Seyferts: $r \gtrsim 100\,\mathrm{pc} \Longrightarrow f \lesssim 10^{-2}$.

Mass:

$$M = \frac{4\pi}{3} f r^3 n_\mathrm{e} m_\mathrm{p} \tag{6.27}$$

$$= 7 \times 10^5\,M_\odot \frac{L_{41}(\mathrm{H}\beta)}{n_3} \tag{6.28}$$

Results: BLR

BLR: Line ratios show RT effects and effects of high density (collisional deexcitation of $n = 2$ level)

$\Longrightarrow$ Lα/H$\beta \sim 5\dots15$ compared to $\gtrsim 30$

Doppler broadening

$$v = \sqrt{\frac{kT}{m_\mathrm{p}}} \sim 10\,\mathrm{km\,s^{-1}}\,T_4^{1/2} \tag{6.29}$$

No observation of [O III] λ4363, 4959, 5007 $\longrightarrow$ ^{1}S$_0$ level of O III deexcited by collisions ("quenching") Since $n_\mathrm{crit} = 10^8\,\mathrm{cm^{-3}} \Longrightarrow n > 10^8\,\mathrm{cm^{-3}}$

On the other hand: C iii] λ1909 visible ($n_\mathrm{crit} = 10^{10}\,\mathrm{cm^{-3}}$)

$\Longrightarrow$ BLR density $n_\mathrm{e} = 10^{8\dots10}\,\mathrm{cm^{-3}}$

Mass and radius using C IV λ1549 line

Results:

$$r = 8L_{42}^{1/2}\ \text{light days} \tag{6.30}$$

$$f = 2.7 \times 10^{-7}\,L_{42}^{-1/2} \tag{6.31}$$

$$M_\mathrm{BLR} = 10^{-3}L_{42}\,M_\odot \tag{6.32}$$

IAAT

Black Hole Paradigm

The Black Hole Paradigm

> Active Galactic Nuclei are powered by supermassive black holes

Alternative solutions to Black Holes are either physically impossible or (at least) very difficult to obtain.

Arguments:

1. Large luminosity of AGN
2. Short term variability of AGN
3. Jets and superluminal motion
4. Physical arguments
5. Occam's Razor

AGN Luminosities

Typical AGN luminosity:

$$L_{\text{AGN}} = 10^{45}\,\text{erg}\,\text{s}^{-1} \tag{6.33}$$

Eddington Luminosity:

$$L_{\text{Edd}} = \frac{4\pi G M m_{\text{p}} c}{\sigma_{\text{T}}} \sim 10^{46} M_8\,\text{erg}\,\text{s}^{-1} \tag{6.34}$$

$\Longrightarrow$ need large mass to radiate below Eddington.

$\Longrightarrow$ Black Hole

Also: efficiency of BH is large (6...42%), i.e., radiation can be produced very efficiently.

AGN Variability, I

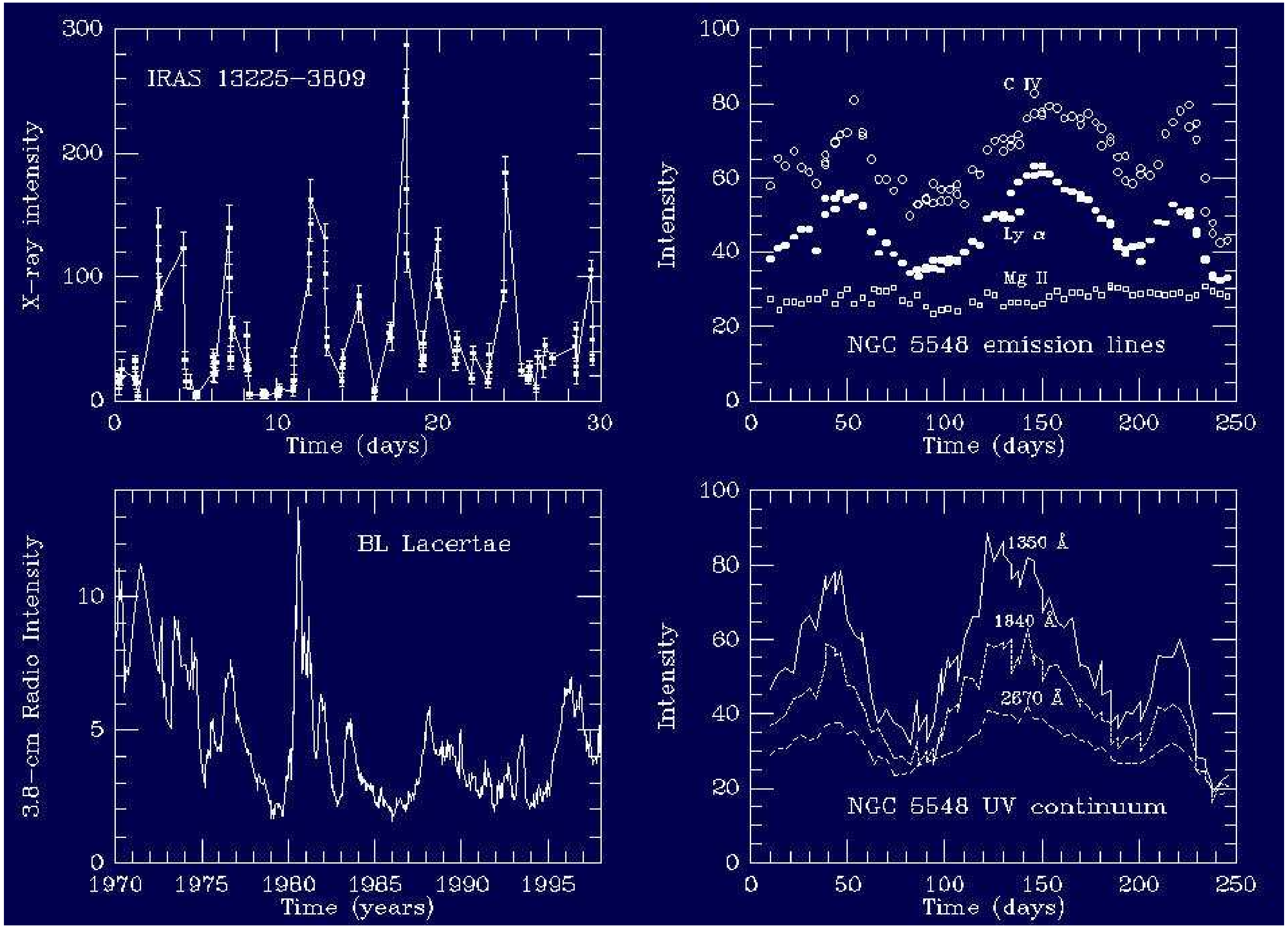

W. Keele

AGN are variable on all timescales

AGN Variability, II

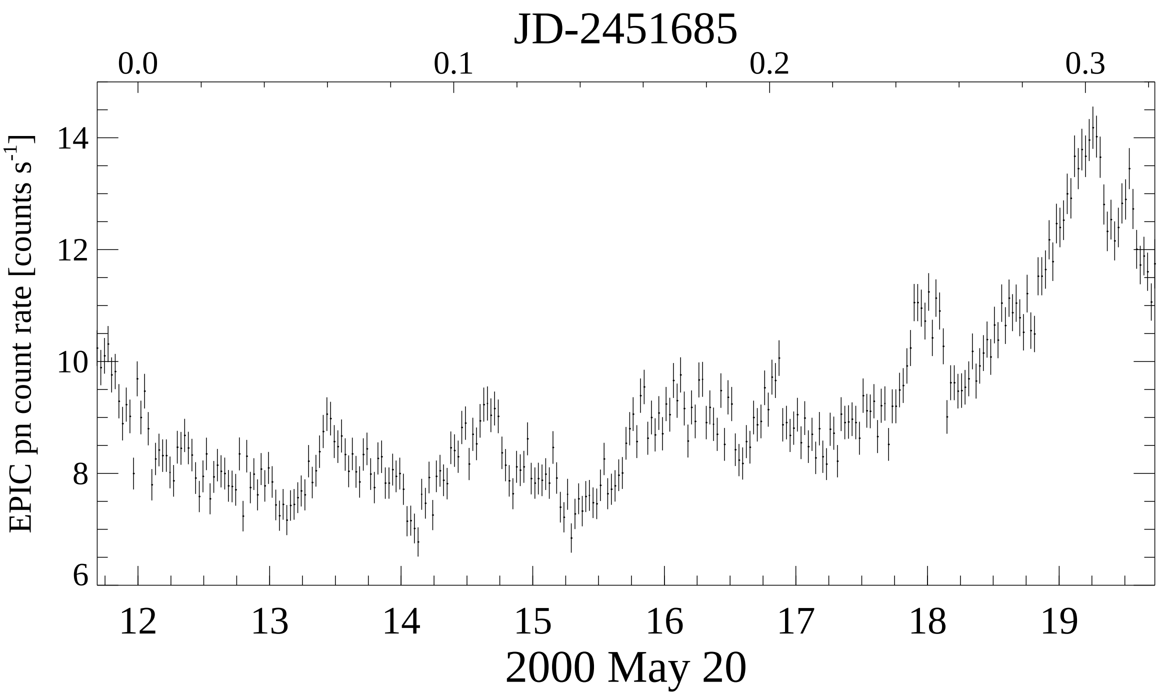

Mkn 766, Benlloch et al., 2001

Short term variability: rapid variability on time-scales shorter than a day or so.

Fastest time-scales: $\Delta t \sim 500\,\text{sec}$. If variation is due to one physical cause (e.g., shock,...) $\Longrightarrow$ upper limit for the size of the emitting region.

$$r_{\text{max}} < c\Delta t \tag{6.35}$$

$\Longrightarrow$ observed luminosity change ΔL occurred within a region smaller than r. Since ΔL is typically large, a large amount of energy is set free in a small region ($r_{\text{max}} \sim 1\,\text{AU}$!) $\Longrightarrow$ Black Hole!

Jets and Superluminal Motion

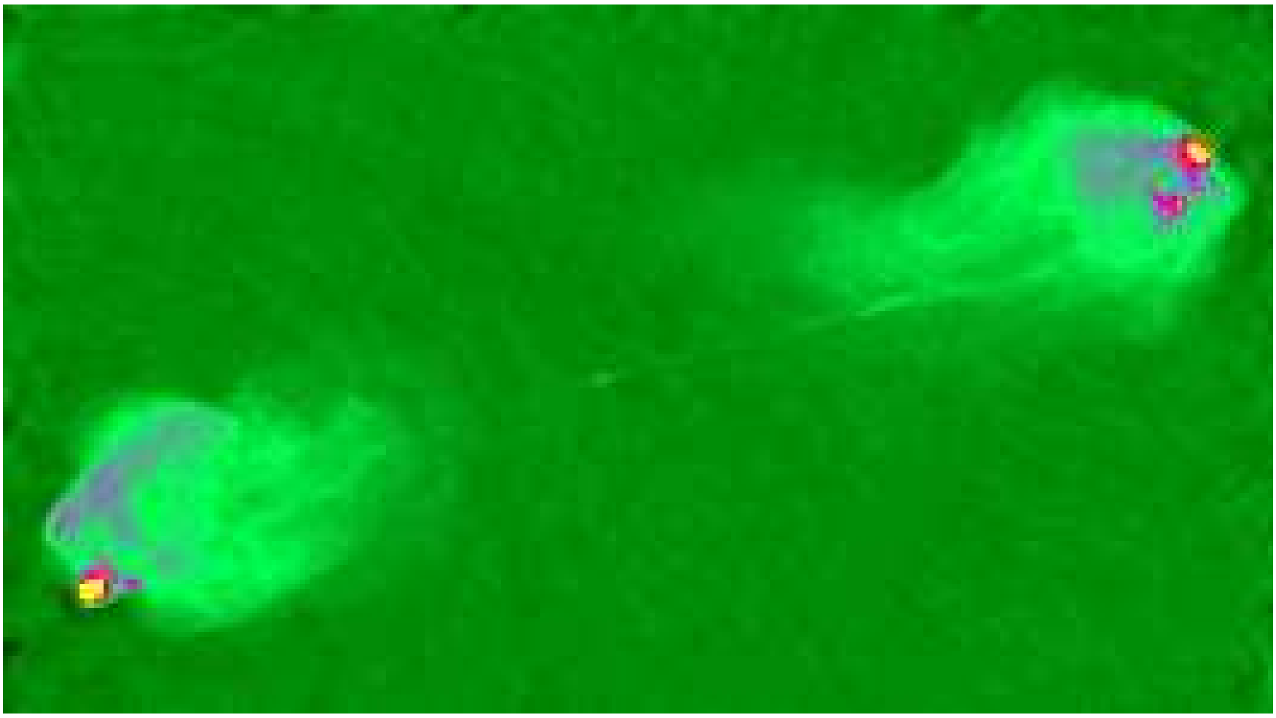

Cygnus A, VLA

Large amounts of energy are needed to generate fast jets. Most efficient mechanism for this is Blandford-Znajek process, which requires (rotating) BH ("Black hole spin paradigm").

In our own galaxy, only BHCs are superluminal sources ("microquasars"), all other jets are weaker and slower (e.g., SS 433, YSOs,...).

Stellar Evolution

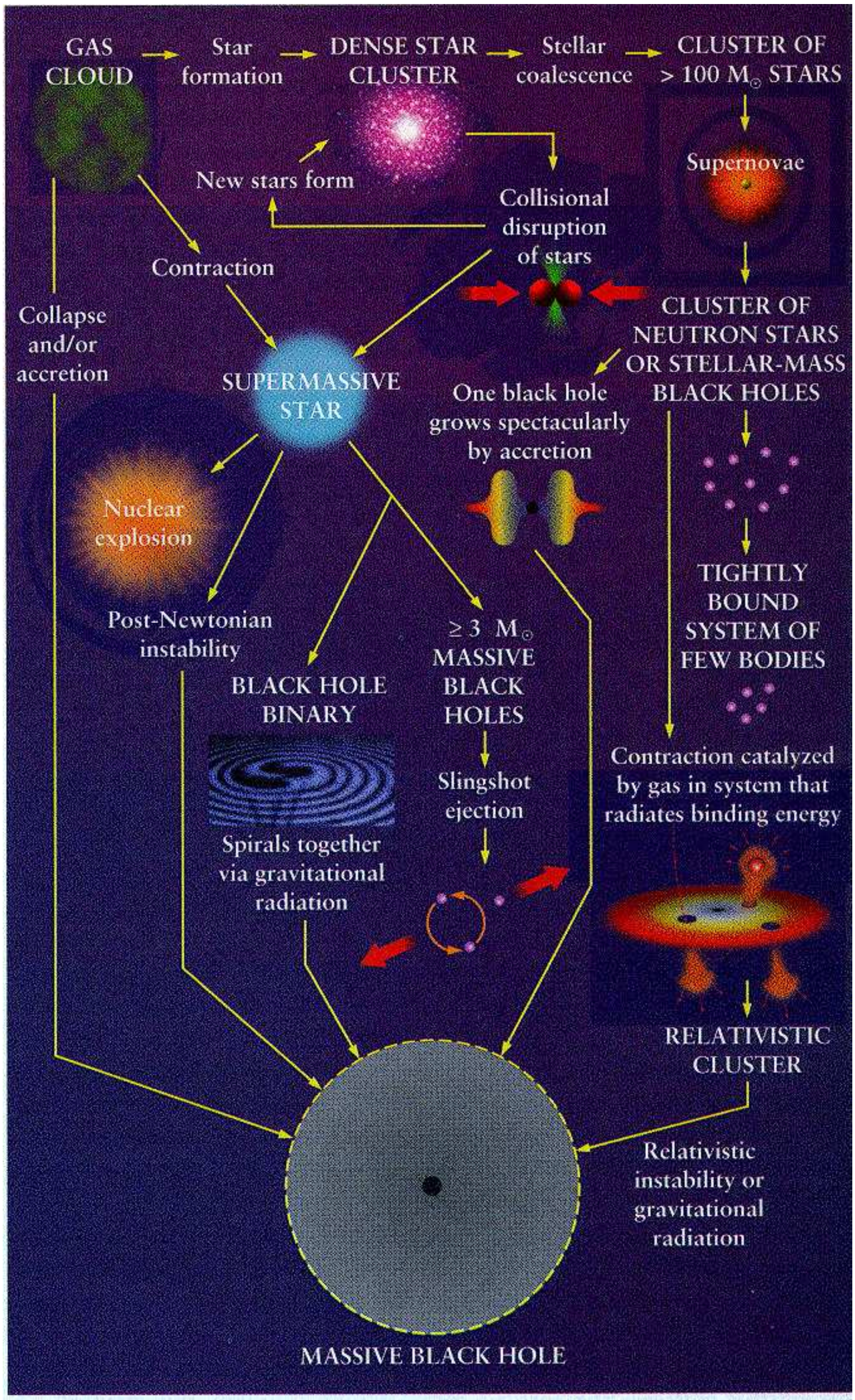

Rees (1984)

Occam's Razor

Wilhelm de Occam ($\sim$1285 – $\sim$ 1350):

"ENTIA NON PRAETER NECESSITATEM MULTIPLICANDA SUNT."

=entities must not be multiplied beyond necessity

"PLURALITAS NON EST PONENDA SINE NECCESITATE"

=plurality should not be posited without necessity.

$\Longleftrightarrow$ Don't make a theory more complicated than necessary

This has also be called the KISS principle:

KISS - Keep It Simple Stupid!

Black holes are the simplest supermassive objects that physics can think of. Realistic BHs can be uniquely characterized by just two properties: Mass and Spin. Why should there be more complicated objects, just to avoid the existence of the singularity?

Direct Methods

Determine presence of Black Hole directly: dynamical mass determination, or determination of presence of horizon.

$\Longrightarrow$ Determine mass from a region that is as small as possible!

$\Longrightarrow$ Determine relativistic effects on spectrum (presence of Schwarzschild or Kerr metric, presence of horizon,. . .)

From the outside to the inside:

2. Gas tori (HST, close AGN, several pc)
1. Stellar motion (galactic center, 1 ly)
3. Water masers (radio, NGC 4258, 0.4 ly)
4. Broadened Iron lines (X-rays, many AGN)

For didactic reasons, will speak about these points in numbered sequence

Galactic Center, I

Velocity profile from point source:

$$v = \sqrt{\frac{GM}{r}} \propto r^{-1/2} \tag{6.36}$$

Distance of GC: $d = 8\,\mathrm{kpc}$, so that

$$\theta = 1'' \Longleftrightarrow r = d\theta = 0.04\,\mathrm{pc} = 0.1\,\mathrm{ly} \tag{6.37}$$

Assuming $M = 10^6\,M_\odot$:

$$v(\theta) \sim 330\,\mathrm{km\,s^{-1}} \tag{6.38}$$

Techniques to determine velocity field:

- High resolution IR spectroscopy (SUSI, 3.5 m NTT)
- High resolution IR imaging (Speckle, 3.5 m NTT, 10 m Keck)

Galactic Center, II

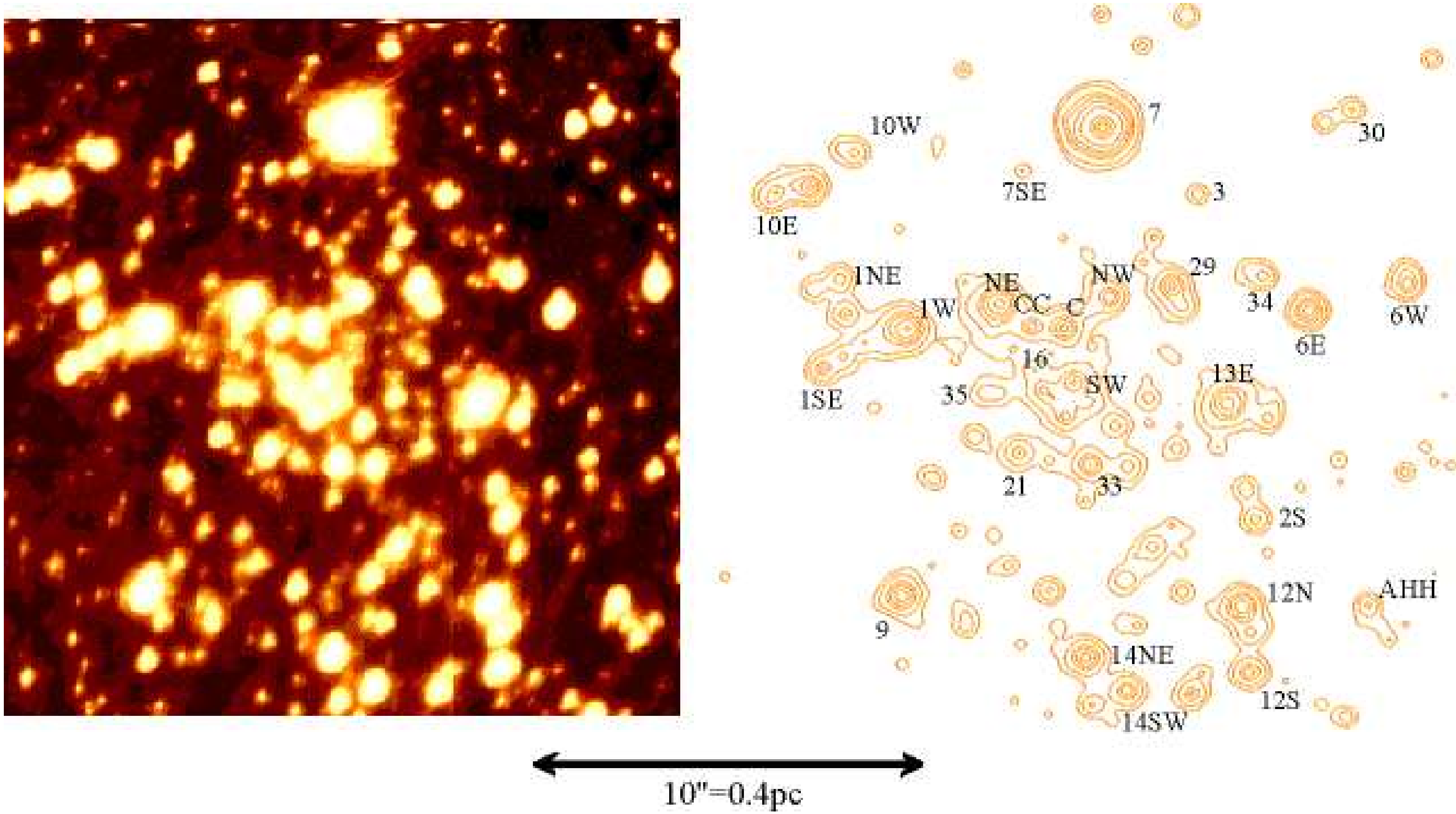

Eckart et al., 1998

Galactic Center, III

More precise determination of velocity profile from radial velocities and proper motion.

- For $\theta \gtrsim 0.1''$: $v \propto \theta^{-1/2}$
- For $1'' < \theta < 5''$ radial velocity profile and proper motions agree

$\Longrightarrow$ No anisotropy in velocity field! Spherical symmetry!

Using these velocities: $M_{\text{GC}} = 2.6 \times 10^6\,M_\odot$

Better masses: Velocity profile from virial theorem:

$$M(r < R) \propto \sum v_i^2 \theta_i \tag{6.39}$$

Galactic Center, IV

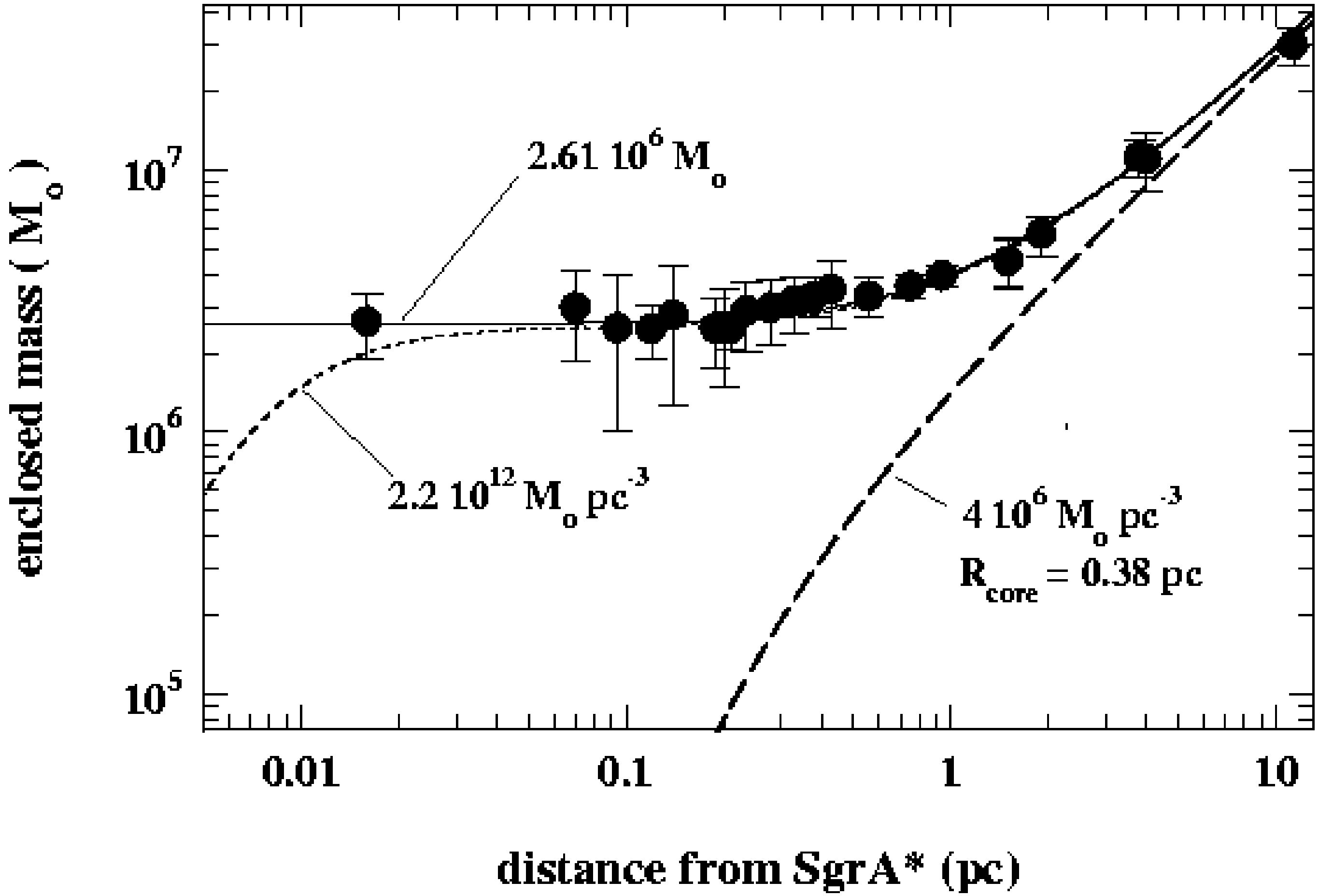

Profile: point-mass with $2.6 \times 10^6\,M_\odot$ *plus* isothermal stellar cluster with $4 \times 10^6\,M_\odot\,\mathrm{pc}^{-3}$, nuclear radius $r = 0.4\,\mathrm{pc}$.

HST Observations of AGN

Same idea as before: measure velocity profile in galaxy, and determine central mass by superposing point mass *plus* model for galaxy potential.

Since it is not possible to determine velocity of individual stars $\Longrightarrow$ measure velocity dispersion σ.

$$\sigma^2 = \frac{GM}{R} \qquad (6.40)$$

Velocity dispersion in galaxy σ_0, therefore *sphere of influence* (i.e., $\sigma > \sigma_0$)

$$R \sim \frac{GM_{\mathrm{BH}}}{\sigma_0^2} \sim 43\,\frac{M_8}{\sigma_{0,100}^2}\,\mathrm{pc} \qquad (6.41)$$

where $\sigma_{0,100} = \sigma_0/100\,\mathrm{km\,s^{-1}}$.
At the distance of the Virgo cluster (20 Mpc): $R \sim 0.2''$, i.e., barely possible with HST.

Nuclear disks, I

Most often shown in HST press releases, which don't make clear difference between these extended ($r \sim 200\,\mathrm{pc}$) disks and the real accretion disk.

Disk are aligned with jets $\Longrightarrow$ coupling galactic disk with inner accretion disk?

It is not clear yet whether nuclear disks can be used to measure black hole mass.

Nuclear disks, II

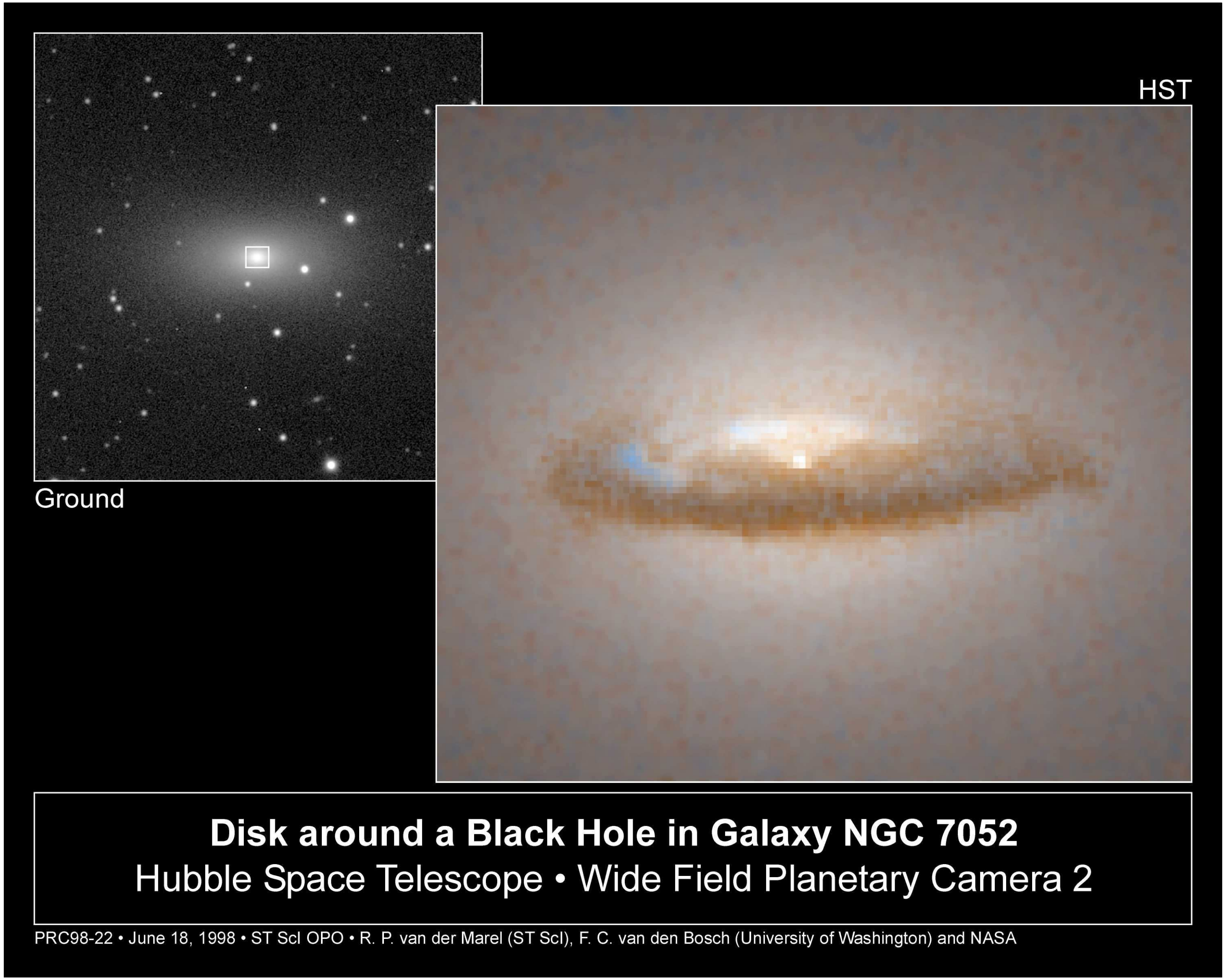

Optical Velocity Profi les, I

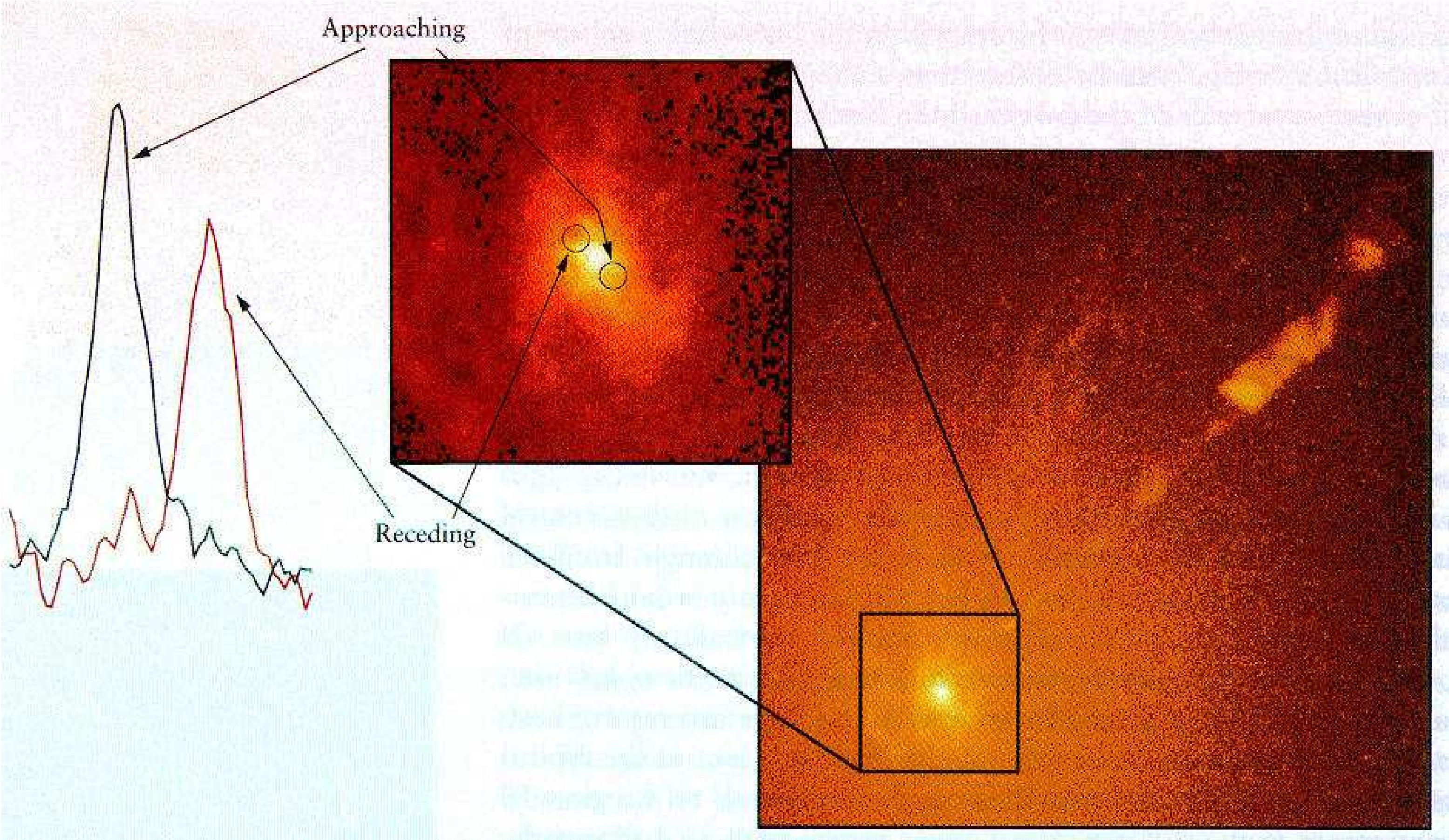

Determine profile from narrow slit line profile. Due to high angular resolution needed, use HST.

Optical Velocity Profi les, II

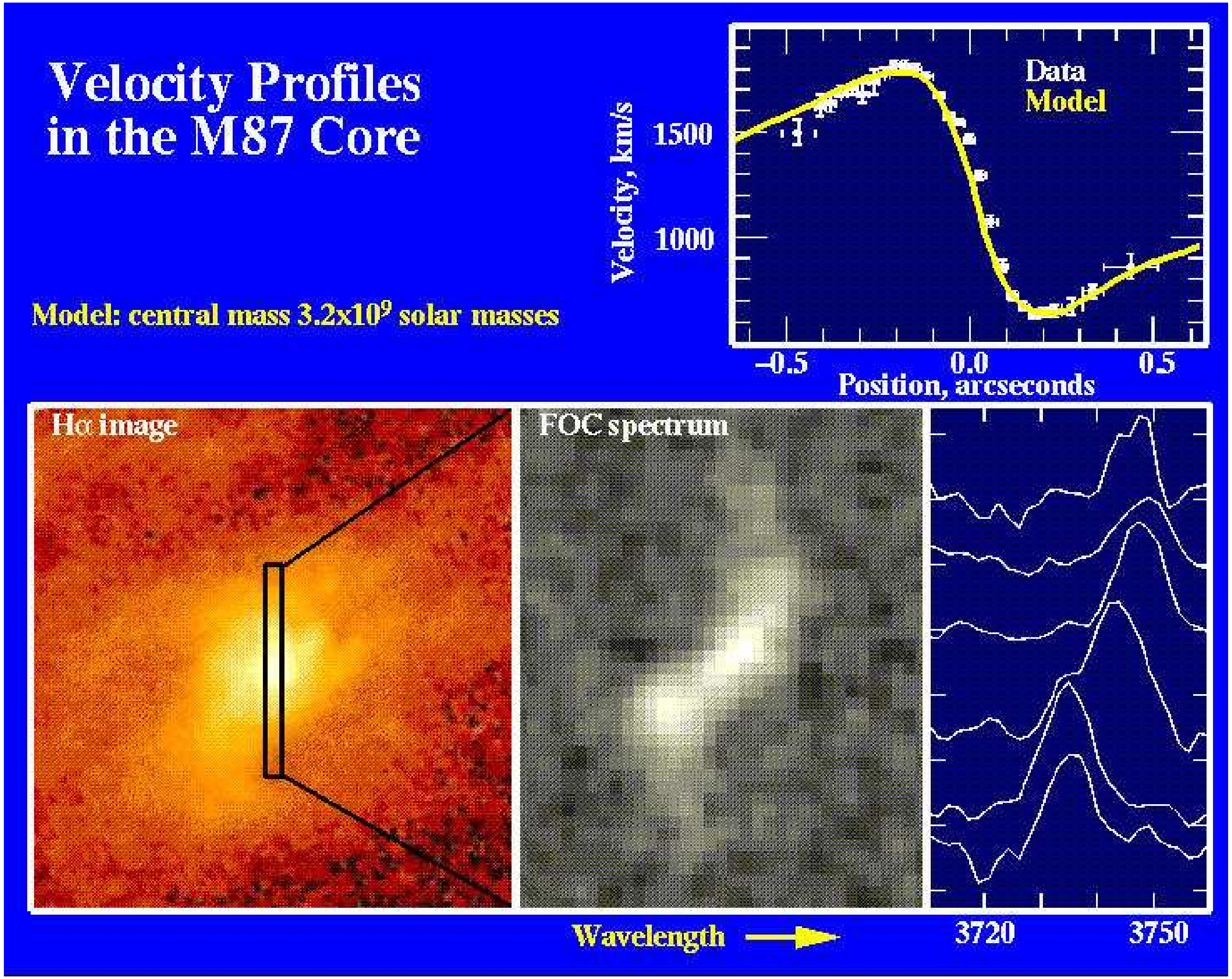

Optical Velocity Profi les, III

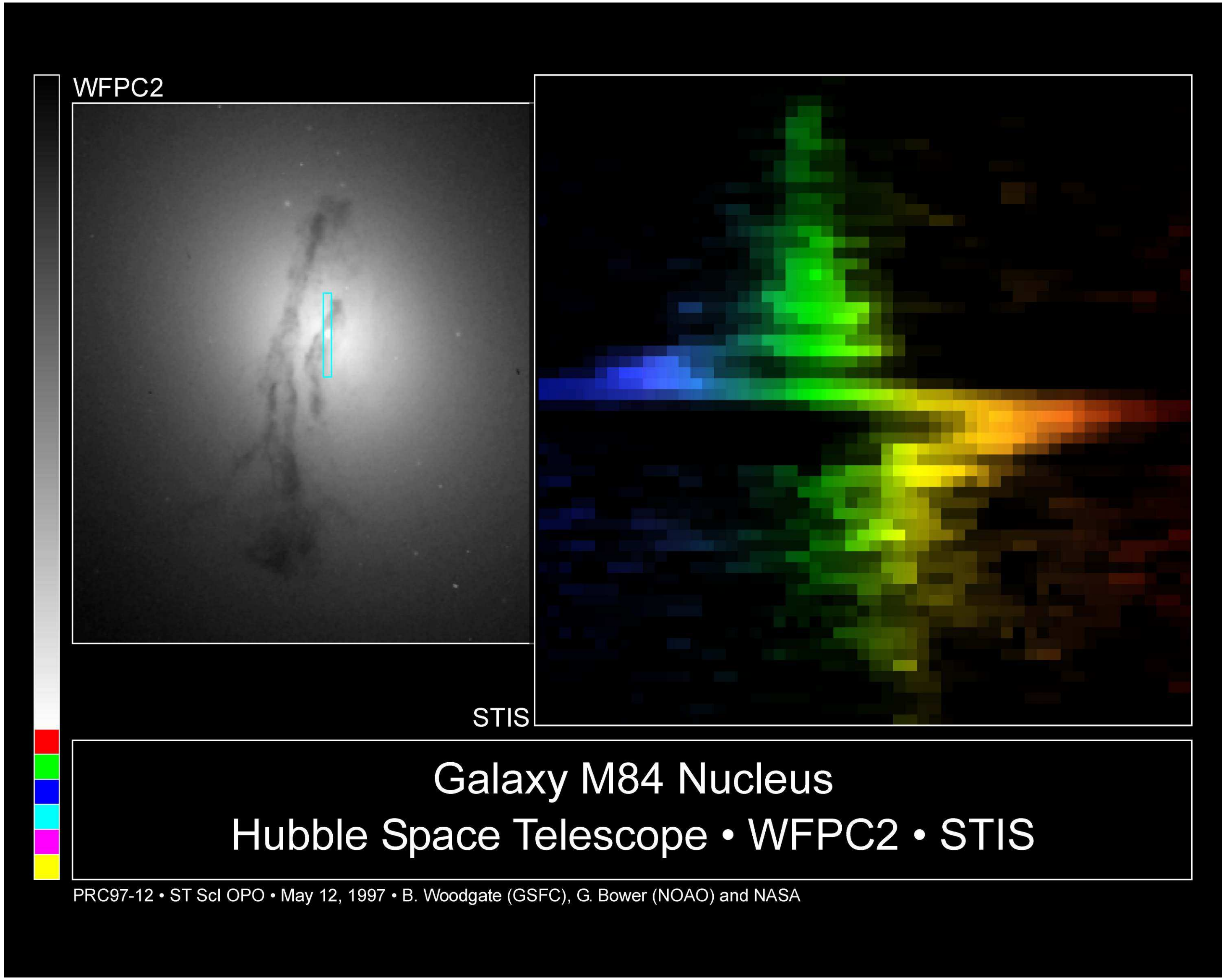

NGC 4258: Water Masers, I

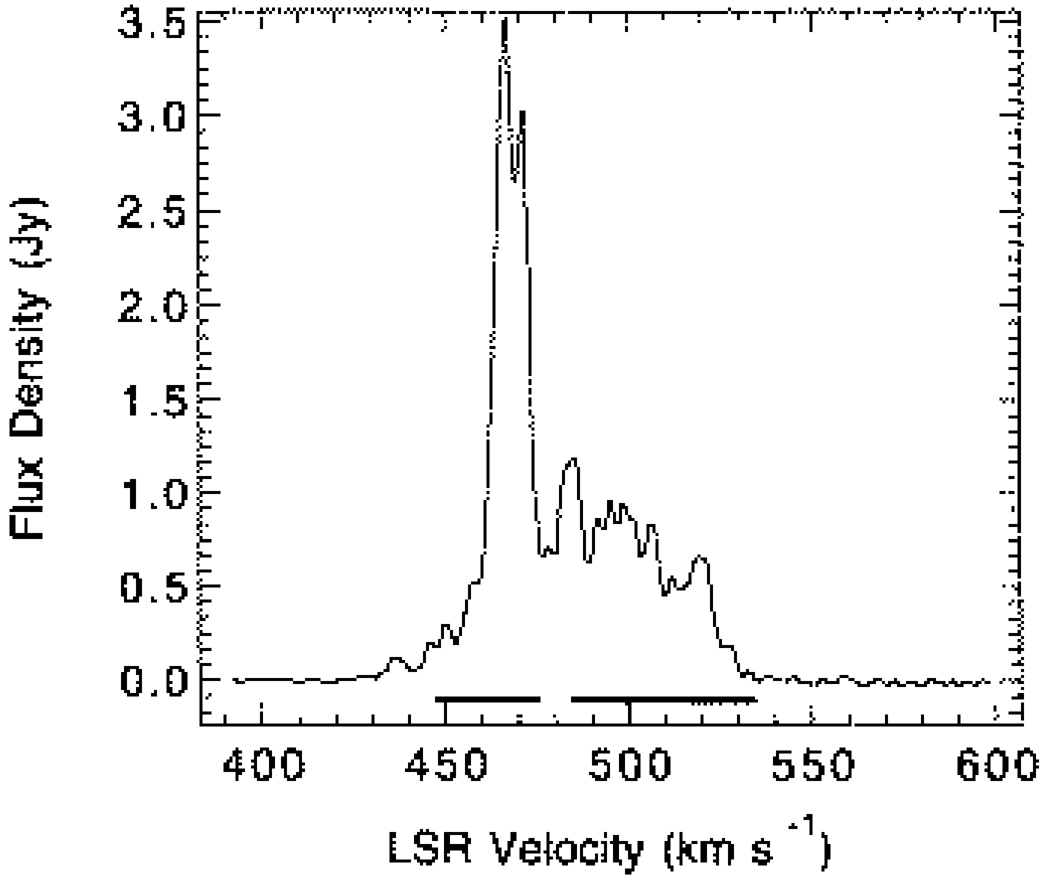

Greenhill et al. (1995)

Narrow radio emission lines produced by water masers in NGC 4258 ($d = 6.5$ Mpc) provide excellent tracers for velocity profile.

Note that the existence of a masing environment is a very rare occurrence in AGN accretion disks.

NGC 4258: Water Masers, II

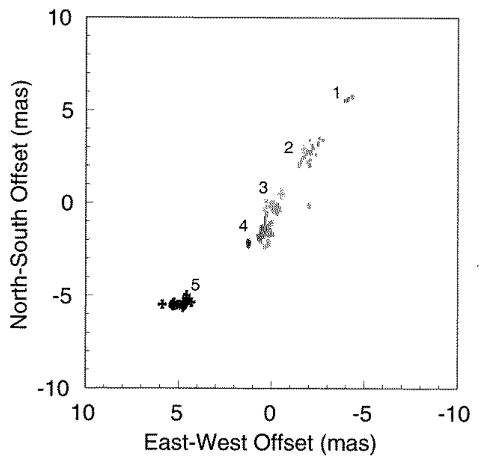

Greenhill et al. (1996); 1 mas $\sim$ 0.03 pc for $d = 6.5$ Mpc

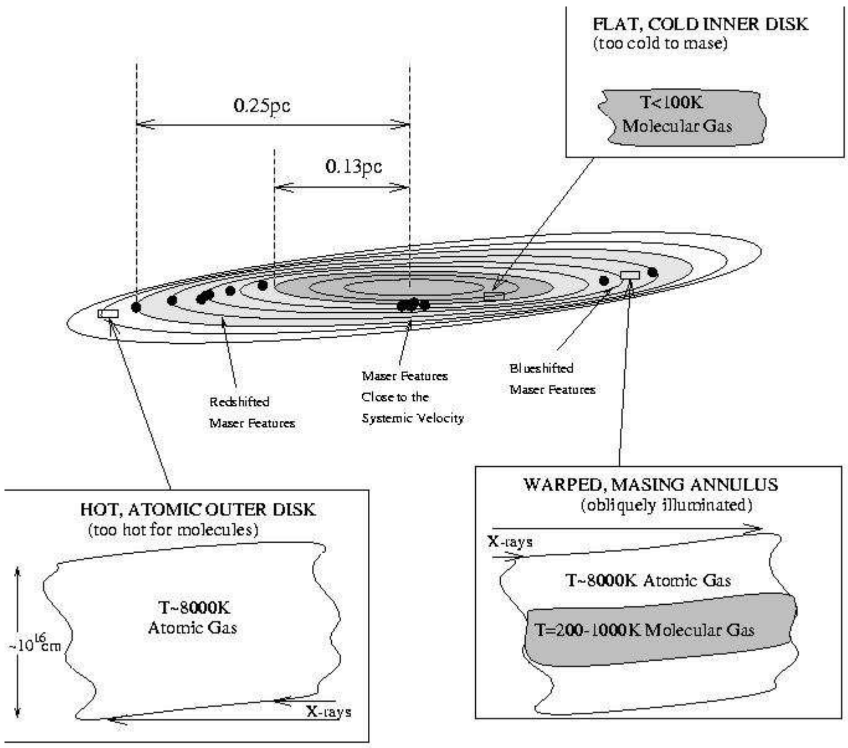

Neufeld & Maloney

Position of masers is along a narrow (almost straight) line $\Longrightarrow$ Evidence for a (warped) accretion disk

IAAT

NGC 4258: Water Masers, III

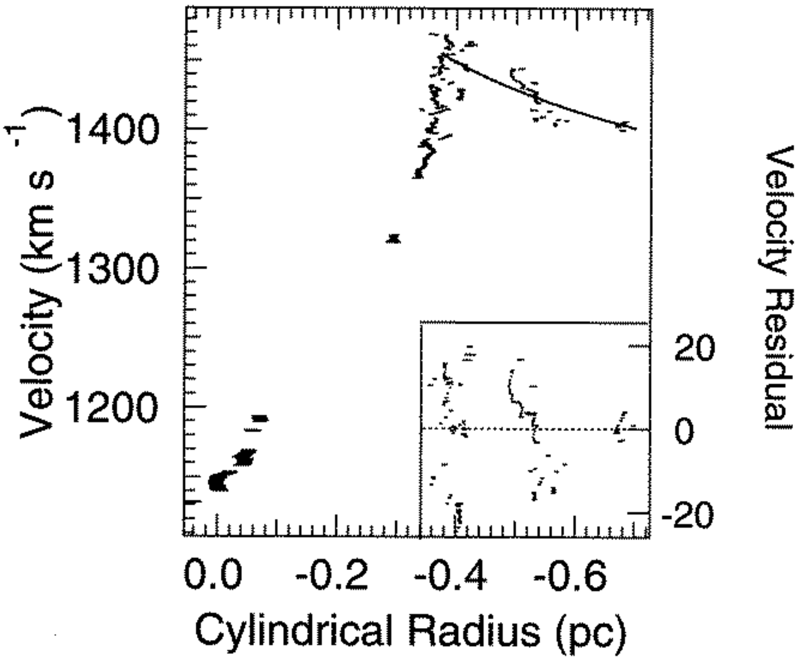

Greenhill et al. (1996)

Velocity-profile measured in the water masers. Accretion disk fitting gives $M_{\text{BH}} \sim 3.6 \times 10^7\,M_\odot$, masers are between 0.12 pc and 0.26 pc, thickness of disk is 3×10^{-4} pc.

Note that there is discussion on nature of accretion flow (ADAF vs. standard α-disk, cf. Neufeld & Maloney (1995)).

NGC 4258: Water Masers, IV

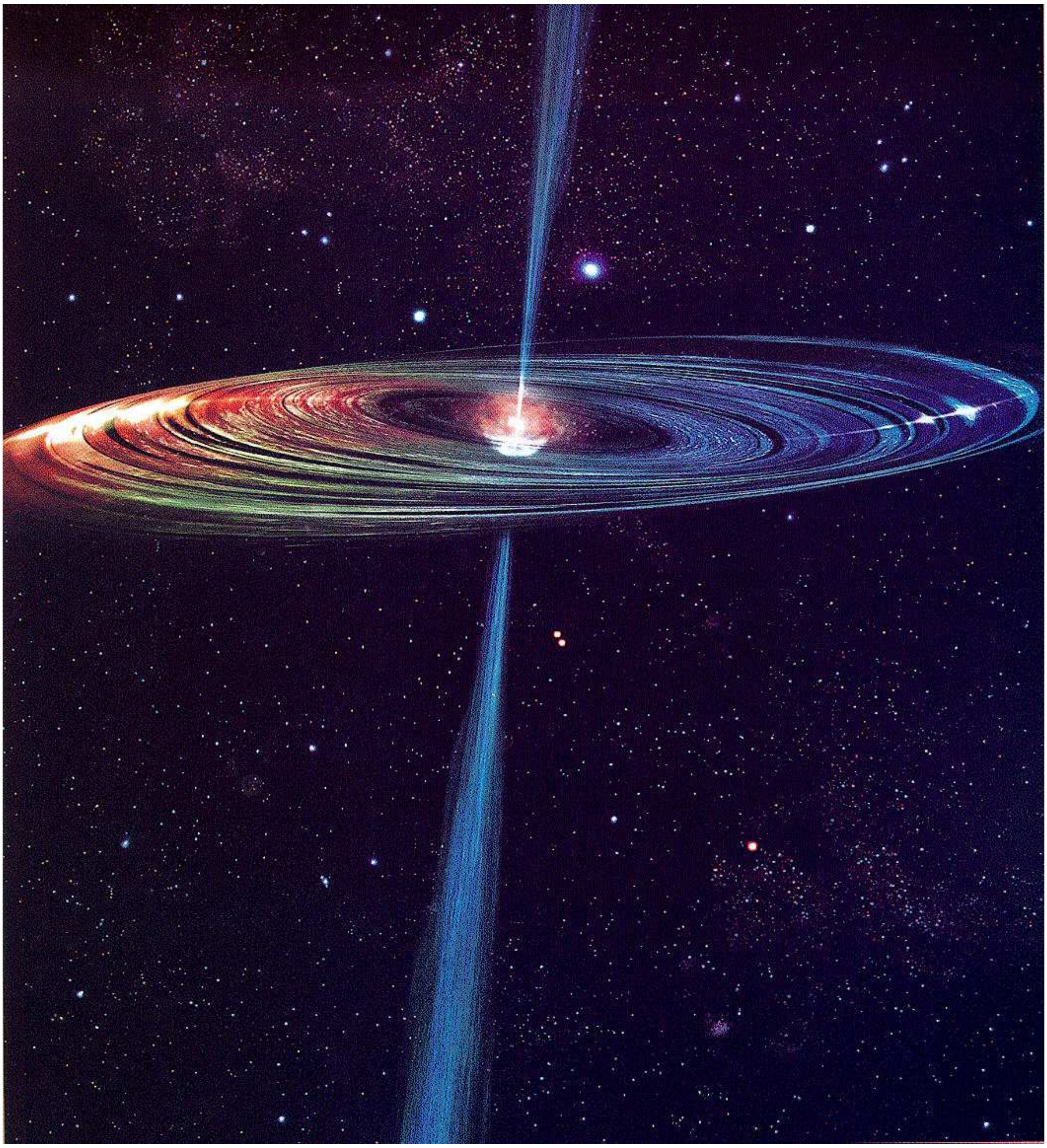

Iron Lines

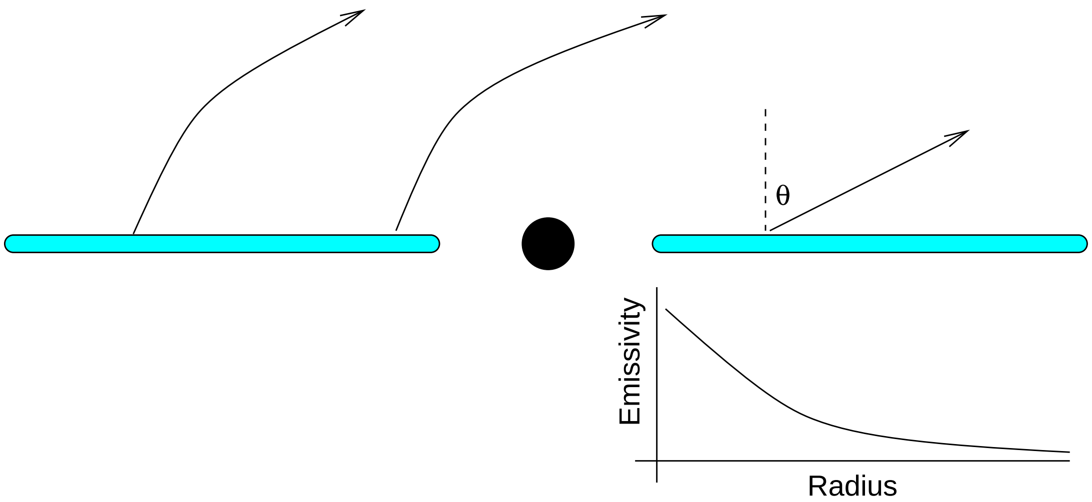

Test GR using fluorescent iron line emission

- Thin accretion disk
- Parameterization of emissivity as $I(r) \propto r^{-\beta}$

Iron Lines

Obtain observed flux by summation over accretion disk:

$$F_{\nu_\mathrm{o}} = \int_\Omega I_{\nu_\mathrm{o}} \cos\theta \,\mathrm{d}\Omega \approx \int_\Omega I_{\nu_\mathrm{o}} \,\mathrm{d}\Omega \tag{6.42}$$

$$= \int_\Omega \frac{I_{\nu_\mathrm{o}}}{\nu_\mathrm{o}^3} \nu_\mathrm{o}^3 \,\mathrm{d}\Omega \tag{6.43}$$

but: $I_{\nu_\mathrm{o}}/\nu_\mathrm{o}^3 = I_{\nu_\mathrm{e}}/\nu_\mathrm{e}^3$ (Liouville)

$$= \int_\Omega \frac{I_{\nu_\mathrm{e}}}{\nu_\mathrm{e}^3} \nu_\mathrm{o}^3 \,\mathrm{d}\Omega \tag{6.44}$$

$$= \int_\Omega g^3 I_{\nu_\mathrm{e}}(r_\mathrm{e}, i_\mathrm{e}) \,\mathrm{d}\Omega \tag{6.45}$$

$$= \iint T(i_\mathrm{e}, r_\mathrm{e}, g) I_{\nu_\mathrm{e}}(r_\mathrm{e}, i_\mathrm{e}) \,\mathrm{d}g \, r_\mathrm{e} \,\mathrm{d}r_\mathrm{e} \tag{6.46}$$

where $T(i_\mathrm{e}, r_\mathrm{e}, g)$ transfer-function (Cunningham, 1975; Speith, Riffert & Ruder, 1995), and $g = \nu_\mathrm{o}/\nu_\mathrm{e} = 1/(1+z)$.

IAAT

Iron Lines

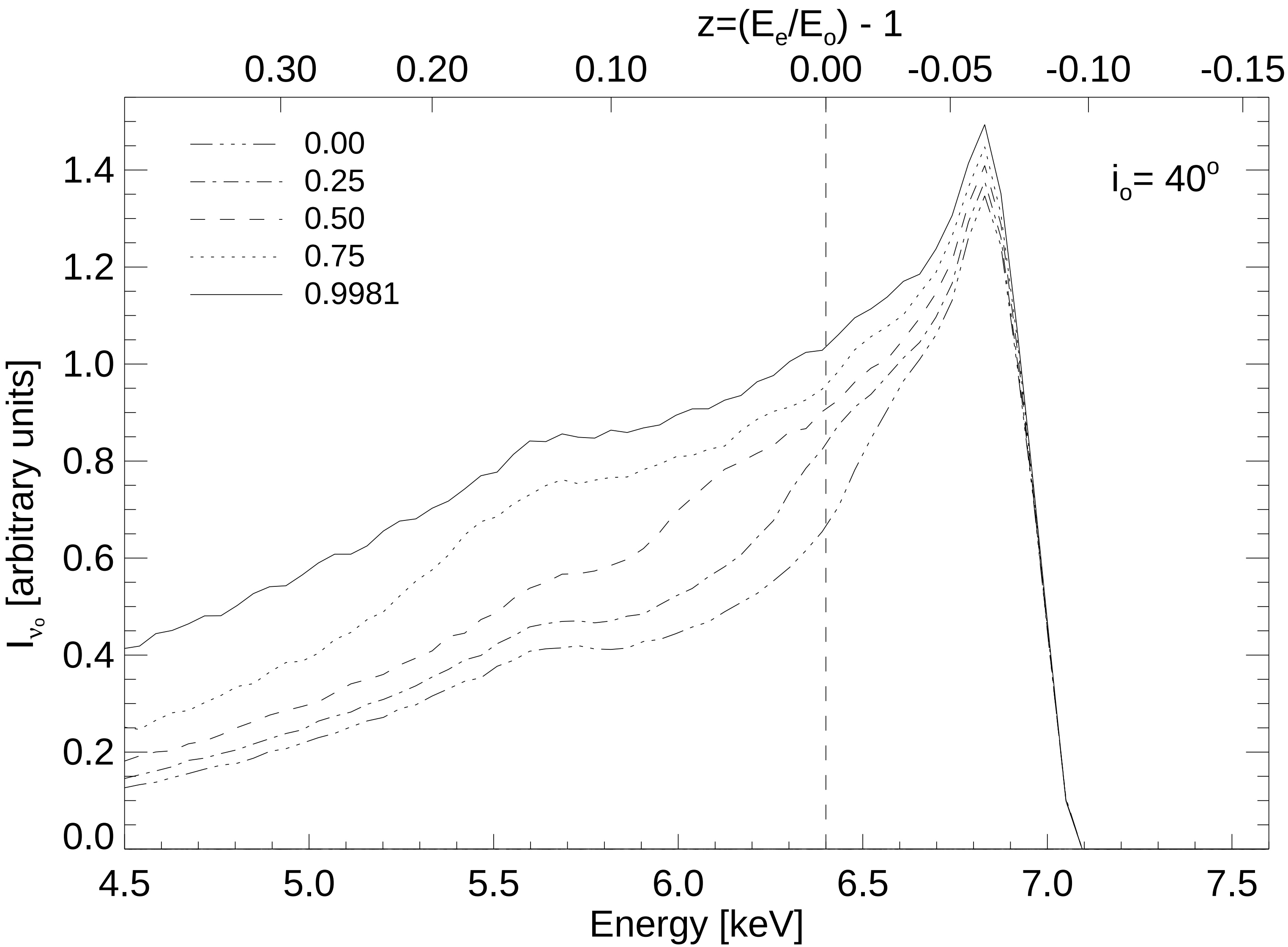

Influence of Angular Momentum

Iron Lines

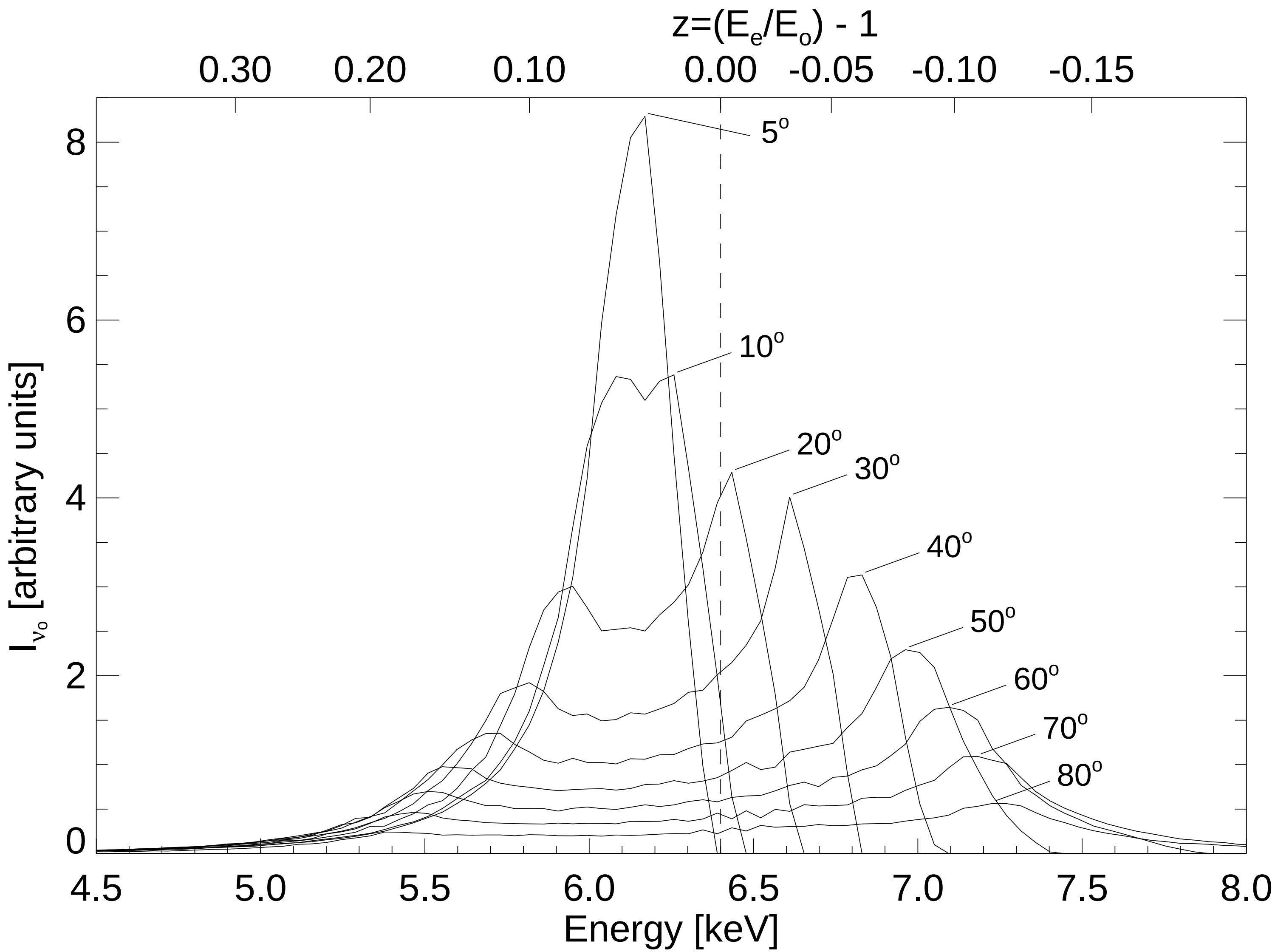

Influence of Inclination

Iron Lines

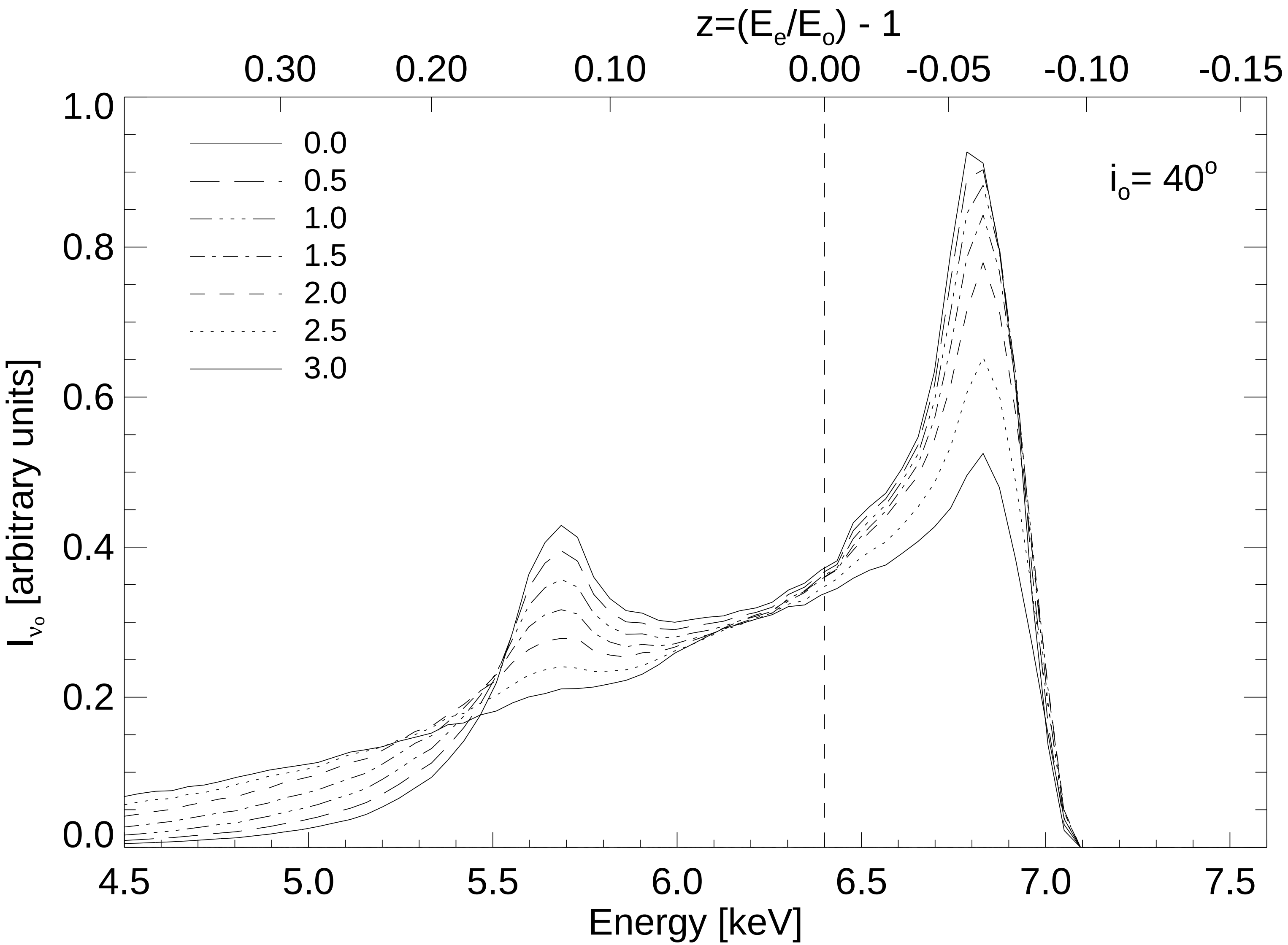

Influence of Emissivity Law ($\epsilon \propto r^{-\beta}$)

Iron Lines

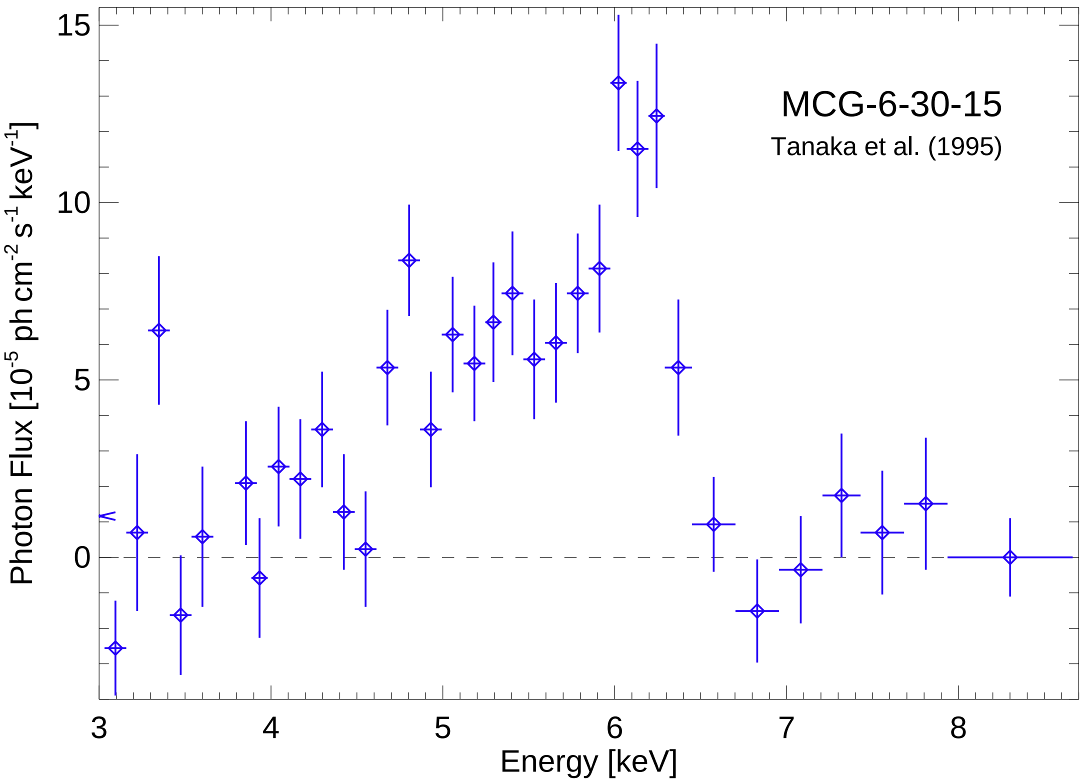

Mean profile of the Fe-Line of MCG −6-30-15
Tanaka et al. (1995)

Iron Lines

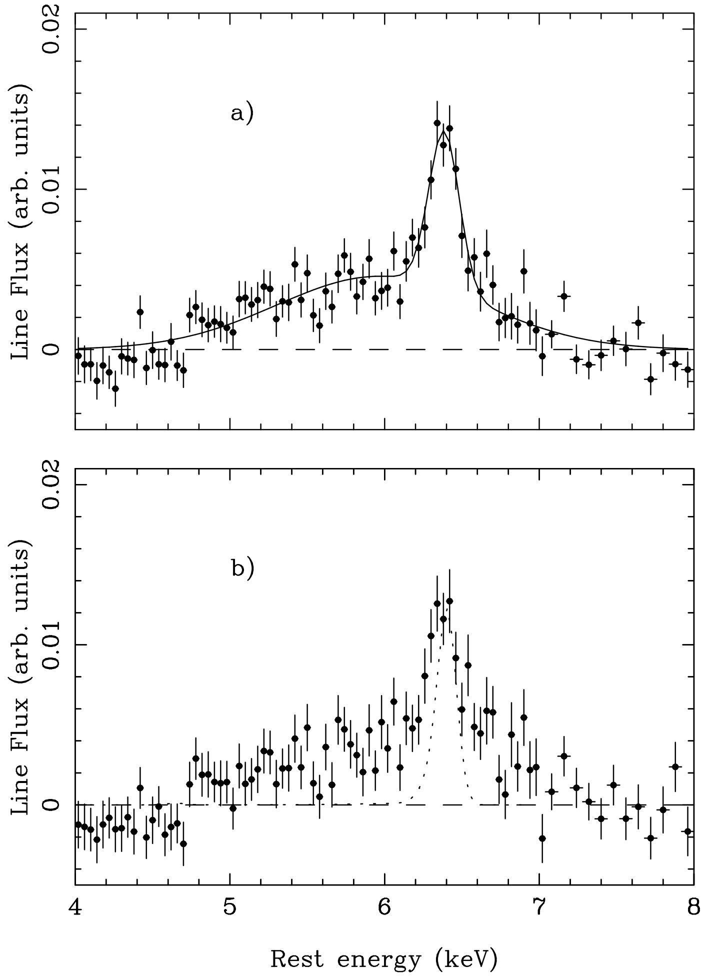

Analysis of ASCA spectra of 18 Sy 1 galaxies, 14 exhibit resolved Kα, FWHM$\sim$ 50000 km/s, most have strong red wing, 8 have $EW \gtrsim 200$ eV.

Nandra et al. (1997)

Iron Lines

- Cold Comptonization: would need $\tau_e > 5$ and low temperature $\Longrightarrow$ not observed in continuum (would require a break at 20 keV).
- Wrong modeling of continuum: "blue wing" could be Fe-edge, but would be at wrong energy (6.5 as compared to 7.1 keV).
- Line blends: wrong form of the line
- Warm absorber: influence negligible
- Wrong assumed geometry: see next slide

Fabian et al. (1995)

Bibliography

Cunningham, C. T., 1975, ApJ, 202, 788

Fabian, A. C., Nandra, K., Reynolds, C. S., Brandt, W. N., Otani, C., Tanaka, Y., Inoue, H., & Iwasawa, K., 1995, MNRAS, 277, L11

Greenhill, L. J., Gwinn, C. R., Antonucci, R., & Barvainis, R., 1996, ApJ, 472, L21

Greenhill, L. J., Jiang, D. R., Moran, J. M., Reid, M. J., Lo, K. Y., & Claussen, M. J., 1995, ApJ, 40, 619

Lawrence, A., 1987, PASP, 99, 309

Nandra, K., George, I. M., Mushotzky, R. F., Turner, T. J., & Yaqoob, T., 1997, ApJ, 477, 602

Neufeld, D. A., & Maloney, P. R., 1995, ApJ, 447, L17

Rees, M. J., 1984, ARA&A, 22, 471

Speith, R., Riffert, H., & Ruder, H., 1995, Comput. Phys. Commun., 88, 109

Tanaka, Y., et al., 1995, Nat, 375, 659

Urry, C. M., & Padovani, P., 1995, PASP, 107, 803